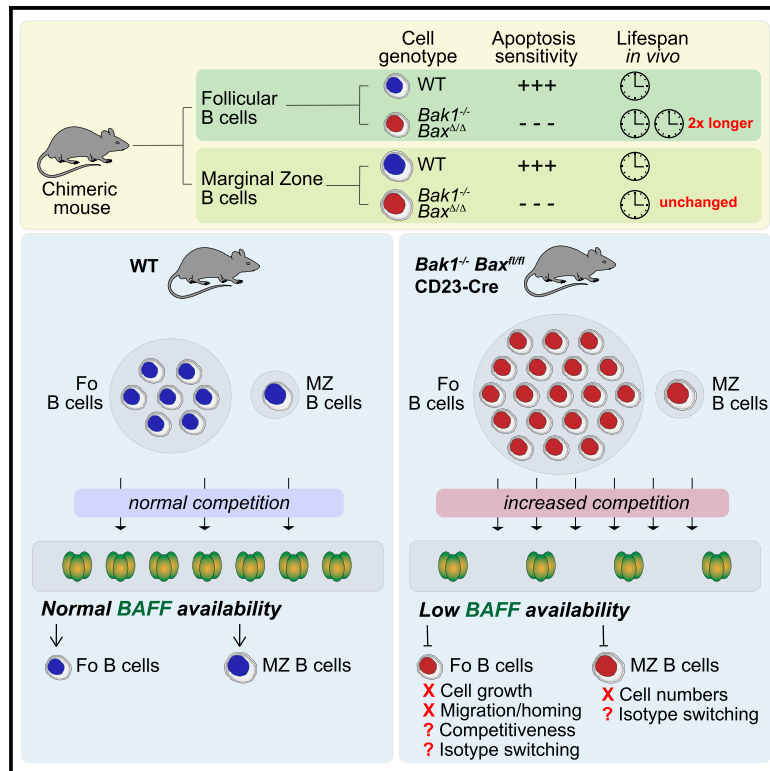


## Homeostatic apoptosis prevents competition-induced atrophy in follicular B cells

### Graphical abstract



### Authors

Stéphane Chappaz, Kate McArthur, Liam Kealy, ..., Kim L. Good-Jacobson, Andreas Strasser, Benjamin T. Kile

### Correspondence

stephane.chappaz@monash.edu (S.C.), benjamin.kile@adelaide.edu.au (B.T.K.)

### In brief

The intrinsic apoptosis pathway is widely considered essential for lymphocyte homeostasis. Here, Chappaz et al. find that intrinsic apoptosis does not regulate marginal zone B cell turnover, yet its disruption in follicular B cells compromises mature B cell physiology by intensifying intercellular competition for BAFF.

### Highlights

- Intrinsic apoptosis controls the lifespan of FoB but not of MZB cells
- Abrogation of apoptosis in mature B cells raises competition for BAFF *in vivo*
- Heightened competition for BAFF compromises the physiology of FoB and MZB cells



## Article

# Homeostatic apoptosis prevents competition-induced atrophy in follicular B cells

Stéphane Chappaz,<sup>1,2,6,12,\*</sup> Kate McArthur,<sup>2,3,6,10</sup> Liam Kealy,<sup>3,4,10</sup> Charity W. Law,<sup>5,6</sup> Maximilien Tailleur,<sup>1</sup> Rachael M. Lane,<sup>1</sup> Anna Lieschke,<sup>7</sup> Matthew E. Ritchie,<sup>5,6</sup> Kim L. Good-Jacobson,<sup>3,4</sup> Andreas Strasser,<sup>6,8</sup> and Benjamin T. Kile<sup>1,2,6,9,11,\*</sup>

<sup>1</sup>Anatomy and Developmental Biology, Monash Biomedicine Discovery Institute, Monash University, Clayton, 3800 VIC, Australia

<sup>2</sup>ACRF Chemical Biology Division, The Walter and Eliza Hall Institute of Medical Research, Parkville, 3052 VIC, Australia

<sup>3</sup>Biochemistry and Molecular Biology, Monash Biomedicine Discovery Institute, Monash University, Clayton, 3800 VIC, Australia

<sup>4</sup>Infection and Immunity Program, Monash Biomedicine Discovery Institute, Monash University, Clayton, 3800 VIC, Australia

<sup>5</sup>Epigenetics and Development Division, The Walter and Eliza Hall Institute of Medical Research, Parkville, 3052 VIC, Australia

<sup>6</sup>Department of Medical Biology, The University of Melbourne, Parkville, 3010 VIC, Australia

<sup>7</sup>Canberra Hospital, Garran, 2605 ACT, Australia

<sup>8</sup>Blood Cells and Blood Cancer Division, The Walter and Eliza Hall Institute of Medical Research, Parkville, 3052 VIC, Australia

<sup>9</sup>Faculty of Health and Medical Sciences, University of Adelaide, Adelaide, 5005 SA, Australia

<sup>10</sup>These authors contributed equally

<sup>11</sup>Present address: Faculty of Health and Medical Sciences, Helen Mayo North Building, Frome Road, University of Adelaide, Adelaide, 5005 SA, Australia

<sup>12</sup>Lead contact

\*Correspondence: [stephane.chappaz@monash.edu](mailto:stephane.chappaz@monash.edu) (S.C.), [benjamin.kile@adelaide.edu.au](mailto:benjamin.kile@adelaide.edu.au) (B.T.K.)

<https://doi.org/10.1016/j.celrep.2021.109430>

## SUMMARY

While the intrinsic apoptosis pathway is thought to play a central role in shaping the B cell lineage, its precise role in mature B cell homeostasis remains elusive. Using mice in which mature B cells are unable to undergo apoptotic cell death, we show that apoptosis constrains follicular B (FoB) cell lifespan but plays no role in marginal zone B (MZB) cell homeostasis. In these mice, FoB cells accumulate abnormally. This intensifies intercellular competition for BAFF, resulting in a contraction of the MZB cell compartment, and reducing the growth, trafficking, and fitness of FoB cells. Diminished BAFF signaling dampens the non-canonical NF- $\kappa$ B pathway, undermining FoB cell growth despite the concurrent triggering of a protective p53 response. Thus, MZB and FoB cells exhibit a differential requirement for the intrinsic apoptosis pathway. Homeostatic apoptosis constrains the size of the FoB cell compartment, thereby preventing competition-induced FoB cell atrophy.

## INTRODUCTION

B lymphocytes are the cellular basis of humoral immunity in higher vertebrates. Two types of mature B lymphocytes are found in mice: B1 cells, which are predominantly located in the peritoneal and pleural cavities, and B2 cells, which reside in secondary lymphoid organs. Mature B2 cells are composed of follicular B (FoB) cells and marginal zone B (MZB) cells, which both arise from transitional B cells, a short-lived, bone marrow (BM)-derived population. In the mouse, FoB cells are circulating cells that live for  $\sim$ 3 months (Förster and Rajewsky, 1990; Rolink et al., 1998) and reside within follicles in the spleen, lymph nodes (LNs), and Peyer's patches. In contrast, MZB cells are sessile, residing in the outer white pulp of the spleen, (Pillai et al., 2005) and they have been proposed to live as long as the host (Hao and Rajewsky, 2001).

Under homeostatic conditions, mature B cell numbers in the mouse are kept relatively constant (Crowley et al., 2008). Each

day, transitional cells enter the pool of mature B cells, replacing (presumably) senescent and/or functionally expended cells that have been cleared. However, the mechanism(s) that regulate the lifespan and clearance of mature B cells *in vivo* remain somewhat ill-defined. While intrinsic apoptosis (for simplicity referred to hereafter as "apoptosis") is thought to play a central role in lymphoid homeostasis, its precise functional contribution in mature B cell homeostasis has never been defined.

The critical step in apoptosis is the activation of two pro-death effector molecules, BAX and BAK, which form pores in the mitochondrial outer membrane, releasing cytochrome c (Youle and Strasser, 2008). This triggers the apoptotic caspase cascade and cell death. In healthy cells, the suppression of apoptotic activity depends on the pro-survival members of the BCL-2 protein family (BCL-2, BCL-XL, BCL-W, MCL-1, and A1), which can physically bind to BAX and BAK, thereby restraining their pro-death activity (Lee et al., 2016). Upon exposure to cellular stress, the levels of pro-apoptotic "BH3-only" proteins (PUMA, NOXA,



BIM, BMF, BAD, BID, HRK, and BIK) are increased and initiate cell death signaling. BH3-only proteins do this by either binding to the pro-survival BCL-2 family members, thereby unleashing BAX and BAK, or by directly activating BAX and BAK (Giam et al., 2008). Cells lacking both BAX and BAK are resistant to pro-apoptotic stimuli; they do not exhibit cytochrome c release or caspase activation, and they are able to maintain clonogenicity (i.e., they can survive and generate viable progeny) (Ke et al., 2018; Lindsten and Thompson, 2006; Wei et al., 2001).

The notion that apoptosis plays an essential role in lymphoid homeostasis dates back to the discovery that the t(14;18) translocation (which deregulates BCL-2 expression) is found at high incidence in follicular lymphoma (Tsujiimoto et al., 1984) and that BCL-2 overexpression confers increased survival capacity (Vaux et al., 1988) and promotes tumorigenesis (Strasser et al., 1990). Decades of research point to a critical role for apoptosis in regulating B cell ontogeny. It is thought to underpin the elimination of cells that have failed to productively recombine the immunoglobulin (Ig) gene locus (Strasser et al., 1994), have assembled a self-reactive B cell receptor (Enders et al., 2003), or have received insufficient cytokine signals (Maraskovsky et al., 1997; Opferman, 2008; Strasser, 2005; Strasser et al., 2008). The idea that apoptosis underpins B cell homeostasis is further supported by the abnormal accumulation of B lymphocytes in mice whose B cell lineage is rendered resistant to apoptosis (Lindsten et al., 2000; McDonnell et al., 1989; Strasser et al., 1990, 1991a; Takeuchi et al., 2005). However, in these mice, the entire lineage (from the progenitor stage onward) was unable to undergo apoptosis, complicating the interpretation of the findings. While early studies demonstrated that resistance to apoptosis protect B cells from cell death for extended periods *in vitro* (Lindsten et al., 2000; McDonnell et al., 1989; Strasser et al., 1990, 1991a, Takeuchi et al., 2005), it is still not clear to what extent it regulates mature B cell lifespan *in vivo*. Moreover, while it has been known for 3 decades that apoptosis-resistant FoB cells are smaller in size relative to wild-type (WT) cells *in vivo* (Sakai et al., 2009; Strasser et al., 1990, 1991b), the underlying mechanism and the significance of this observation have yet to be understood. Furthermore, the MZB cell compartment is reduced in mice in which the B cell lineage cannot undergo apoptosis (Sakai et al., 2009; Takeuchi et al., 2005), a counterintuitive result yet to be fully explored.

Two crucial signals regulate mature B cell survival: those emanating from the B cell antigen receptor (BCR) (Lam et al., 1997), and those transduced through the receptor for the tumor necrosis factor-family member, B cell-activating factor (BAFF). Patients carrying mutations in the gene encoding BAFF receptor (BAFF-R) suffer from B lymphopenia and agammaglobulinemia and exhibit impaired humoral immune responses (Smulski and Eibel, 2018; Warnatz et al., 2009), illustrating the essential role of BAFF in B cell homeostasis. In mice, the loss of BAFF signaling does not perturb B lymphopoiesis in the BM, but severely decreases the numbers of transitional, FoB, and MZB cells (Sasaki et al., 2004; Schiemann et al., 2001; Shulga-Morskaya et al., 2004). The homeostatic role of BAFF in B cells is linked to its pro-survival activity in peripheral B cells. Mature B cells fail to survive in the absence of BAFF-R signaling, both *in vitro* or *in vivo* (Rauch et al., 2009; Rolink et al., 2002; Woodland et al., 2008),

and a spontaneous mutation in the gene encoding BAFF-R severely truncates the lifespan of FoB cells (Harless et al., 2001).

BAFF is thought to promote B cell survival by antagonizing apoptosis (Opferman, 2008; Strasser, 2005). BAFF increases the expression of pro-survival MCL-1, BCL-2, BCL-XL, and A1 in B cells (Do et al., 2000; Hsu et al., 2002; Jacque et al., 2015; Woodland et al., 2008) and reduces that of pro-apoptotic BAK and BIM (Craxton et al., 2005; Do et al., 2000). This anti-apoptotic activity has also been linked to lymphoid malignancies, as it is produced in an autocrine fashion by non-Hodgkin lymphoma, chronic lymphocytic leukemia, and multiple myeloma cells and protects malignant cells from apoptosis *in vitro* (He et al., 2004; Kern et al., 2004; Moreaux et al., 2004; Novak et al., 2002, 2004). However, BAFF is likely to exert functions beyond blocking apoptosis, as BCL-2 overexpression cannot rescue mature B cell compartments in mice in which BAFF-R signaling is disrupted (Rahman and Manser, 2004; Sasaki et al., 2004; Tardivel et al., 2004). These data are difficult to interpret, because, on the one hand, BCL-2 overexpression may not completely suppress BAX and BAK activity, and on the other hand, BCL-2 has been postulated to exert non-apoptotic functions (Gross and Katz, 2017), although this is controversial (Delbridge et al., 2016).

BAFF exhibits many of the biological activities that are characteristic of archetypal growth factors. It activates several signaling pathways, including those involving AKT, mechanistic target of rapamycin (mTOR), and phosphatidylinositol 3-kinase (PI3K) (Jacque et al., 2015; Otipoby et al., 2008; Patke et al., 2006; Woodland et al., 2008), promotes RNA and protein synthesis, and increases protein content and cell size (Patke et al., 2006; Woodland et al., 2008). BAFF induces profound transcriptional changes in B cells (Almaden et al., 2014; De Silva et al., 2016) activating the non-canonical nuclear factor  $\kappa$ B (NF- $\kappa$ B) (Claudio et al., 2002; Kayagaki et al., 2002) and to a lesser extent the canonical NF- $\kappa$ B pathway (Enzler et al., 2006).

The cellular source of BAFF that sustains B cell homeostasis is a radioresistant population of fibroblastic reticular cells (FRCs) residing within B cell follicles (Cremasco et al., 2014; Gorelik et al., 2003). Artificially raising BAFF levels is sufficient to enlarge mature B cell compartments in mice (Mackay et al., 1999; Wilhelmson et al., 2018), demonstrating that the amount of BAFF produced under homeostatic conditions is limiting and constrains peripheral B cell numbers.

To investigate the role of apoptosis in mature B cell homeostasis, we generated conditional knockout (cKO) mice in which FoB and MZB cells lack both *Bax* and *Bak1*. We found that apoptosis regulates the *in vivo* lifespan of FoB cells, but not that of MZB cells, indicating that MZB cell turnover is regulated by as-yet-unknown mechanisms. In the spleen of cKO mice, FoB cell numbers double by 10 weeks of age. This leads to increased intercellular competition for BAFF, compromising the size of the MZB cell compartment, and aspects of FoB cell biology, such as cell growth, trafficking, and competitiveness. Augmenting BAFF levels in cKO mice was sufficient to restore MZB cell numbers and FoB cell growth and trafficking. These results demonstrate that a central function of apoptosis in FoB cell homeostasis is to restrain intercellular competition for BAFF.

## RESULTS

### Deletion of *Bax* and *Bak1* increases the lifespan of FoB cells but not MZB cells

To examine the role of apoptosis in mature B cell homeostasis, we generated mice in which only mature B cells lacked the essential apoptosis effectors BAX and BAK. Mice carrying a germline deletion of *Bak1* were inter-crossed with animals harboring a conditional allele of *Bax* and the CD23-cre transgene (Tg, the latter being expressed from the transitional B cell stage onward) (Kwon et al., 2008). We examined the efficiency of *Bax* gene deletion in transitional, FoB and MZB cells purified from cKO mice and their littermates (Figure S1A). The deleted *Bax* allele could be detected in cKO cells from the T1 compartment onward (Figure S1B). The non-excised *Bax* allele could be amplified in T1 and T2 cells from cKO mice, but was undetectable in FoB and MZB cells (Figure S1B), indicating that deletion of the conditional *Bax* allele was nearly complete in mature B cells. Accordingly, FoB and MZB cells isolated from cKO mice were resistant to pharmacological inhibition of BCL-2, BCL-XL, and BCL-W with the BH3 mimetic drug ABT-737 (Oltersdorf et al., 2005) (Figure S1C) and remained viable when subjected to growth factor deprivation (GFD) (Figures S1D–S1G). These results demonstrate that the deletion of the conditional *Bax* allele is complete in both FoB and MZB cells of cKO mice and that these cells are consequently protected from apoptosis.

We next examined the role of apoptosis in the control of the lifespan of mature B cells. To directly compare the lifespan of WT and cKO mature B cells in the same environment, we generated mixed BM chimeras in which recipient, donor cKO (test), and WT (competitor) cells carried distinct allelic combinations of the Ly5 congenic marker (Figure 1A). Lineage<sup>-</sup> cKO BM was isolated from 6 individual cKO mice, and each BM suspension was mixed with a unique suspension of lineage<sup>-</sup> WT BM cells at a 1:9 ratio and transferred into irradiated WT recipients (Figure 1A). The recipients were then administered bromodeoxyuridine (BrdU) for 6 consecutive weeks—a pulse period allowing the labeling of donor-derived mature B cells. The biological replicates were analyzed at 7 different time points between 20 and 70 days of chase. Flow cytometric analysis allowed the resolution and quantification of BrdU<sup>+</sup> cells among mature B cells of both test and competitor origin (Figure 1B). Consistent with previous findings (Förster and Rajewsky, 1990; Rolink et al., 1998), WT FoB cells had a lifespan of ~88 days (Figure 1C). The lifespan of cKO FoB cells increased to 172 days, and their representation within the BrdU<sup>+</sup> FoB cell population increased accordingly over the 7 weeks of our analysis (Figure 1D). Hence, the inhibition of apoptosis confers a robust survival advantage to FoB cells. In contrast, the lifespan of cKO MZB cells was identical to their WT counterparts (Figure 1E), and their representation within the BrdU<sup>+</sup> compartment did not change over time (Figure 1F). These data indicate that mature B cell subsets have a differential requirement for apoptosis in regulating their *in vivo* lifespan.

### Disruption of mature B cell apoptosis *in vivo* increases intercellular competition

To further dissect the role of apoptosis in mature B cell homeostasis, we analyzed cKO mice and *Cre*<sup>-</sup> littermates. At 6 weeks

of age, mature B cells in cKO animals were normal in terms of numbers and cell size (Figures S2B–S2E) but expressed lower levels of CD21 compared to control cells (Figures S2A and S2F). Moreover, the FoB:MZB cell ratio was significantly increased in 6-week-old cKO mice (Figure S2G). By 10 weeks of age, CD21 expression remained low in cKO FoB cells (Figure S2H), but this did not prevent the identification of mature B cells residing in secondary lymphoid organs and BM (Figures 2A and 2B). FoB cell numbers were doubled in the spleen of cKO mice (Figure 2C) and trended toward an increase (without reaching significance) in LNs (Figure 2D). Recirculating FoB cell numbers were also doubled in the BM (Figure 2E). As previously reported (Sakai et al., 2009; Takeuchi et al., 2005), the numbers of MZB cells were reduced in cKO mice by 10 weeks of age (Figure 2C) and their representation within mature B cells further decreased (Figures S2I and S2J). Of note, the size of cKO FoB cells in 10-week-old animals was decreased compared to controls in the spleen, LNs, and BM (Figures 2F–2H). This phenomenon, called atrophy, occurs in lymphocytes deprived of growth factors *in vitro* (Rathmell et al., 2000; Woodland et al., 2008) and for as-yet-unknown reasons in *Bcl-2* Tg B cells *in vivo* (Sakai et al., 2009; Strasser et al., 1990, 1991b). Atrophy was not observed in FoB cells in 6-week-old cKO mice (Figures S2D and S2E), indicating that it is not an intrinsic property of apoptosis-resistant B cells.

We hypothesized that atrophy may result from an increase in competition among mature B cells due to the gradual expansion of the FoB cell compartment over time. To test this hypothesis, we reduced competition in 10-week-old cKO mice by depleting B cells with specific antibodies (Figure 2I). Depletion reduced the numbers of mature B cells in the spleen, LNs, and BM (without reaching statistical significance) (Figure 2J), and this restored mature B cell size in all organs (Figure 2K). This was specific to the B cell compartment as neither the number (Figure 2L) nor the size (Figure 2M) of CD4 T cells were affected in cKO mice. These data demonstrate that homeostatic turnover via the intrinsic apoptosis pathway constrains the numbers of FoB cells, preventing competition-induced atrophy.

### BAFF is the limiting factor that restricts the number and size of mature B cells

We reasoned that reduced cell death compromises the health of the FoB cell population by increasing competition for a B cell-specific factor. Given its pivotal role in peripheral B cell homeostasis and its ability to regulate CD21 expression (Gorelik et al., 2004), BAFF seemed a likely candidate. Consistently, we found that the levels of BAFF were significantly decreased in the serum of cKO animals from 5 to 6 weeks of age (Figure 3A). Importantly, raising BAFF availability in cKO mice via injection of recombinant protein was sufficient to restore FoB cell size (Figures 3B and 3C). We wondered whether in mice with mature B cells resistant to apoptosis, alleviating competition for BAFF for a sustained period of time could further increase the size of the FoB cell population and restore the MZB cell compartment. To test this, we reconstituted lethally irradiated mice expressing a BAFF Tg expressed in the radioresistant compartment with BM cells from WT, cKO, or *Cre*<sup>-</sup> donors (Figure 3D). Eight weeks after transplantation, the number of MZB cells derived from cKO donors

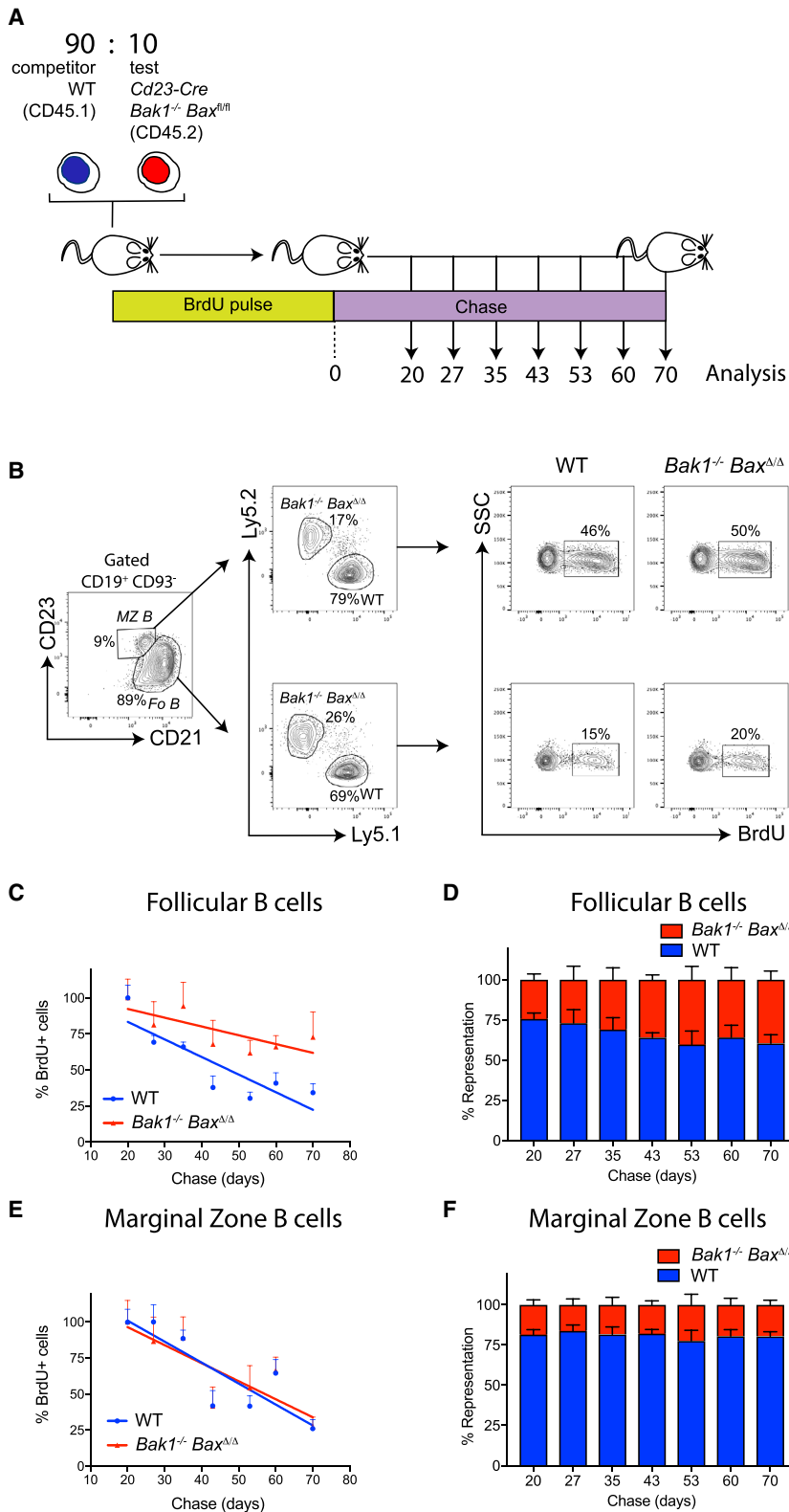


**Figure 1. Co-deletion of *Bax* and *Bak1* in mature B cells extends FoB cell lifespan but does not alter the survival of MZB cells**

(A) Mixed BM marrow chimeras were generated by transplanting a 9:1 ratio of Ly5.1<sup>+</sup> WT lineage<sup>-</sup> competitor BM cells and Ly5.2<sup>+</sup> cKO test cells, respectively, into lethally irradiated Ly5.1<sup>+</sup> Ly5.2<sup>+</sup> recipients (6 biological replicates). Chimeras were fed BrdU for 6 weeks (Pulse). The quantification of BrdU<sup>+</sup> B cells was done 20, 27, 35, 43, 53, 60, and 70 days after the end of BrdU administration (Chase).

(B) Gating strategy to quantify BrdU<sup>+</sup> FoB and MZB cells from WT and cKO origin.

(C) Lifespan curves of BrdU<sup>+</sup> FoB cells. Data show means  $\pm$  SEMs (n = 6/time point). Average number of BrdU<sup>+</sup> cells at day 20 was set at 100%. Cell lifespan estimates obtained from linear regression analysis: WT cells: 88 days, cKO cells: 172 days.

(D) Representation of WT cells and cKO cells within BrdU<sup>+</sup> FoB cells as a function of time.

(E) Lifespan curves of BrdU<sup>+</sup> MZB cells. Data show means  $\pm$  SEMs (n = 6/time point). Lifespan estimates: WT cells: 92 days, cKO cells: 101 days.

(F) Representation of WT cells and cKO cells within BrdU<sup>+</sup> MZB cells as a function of time. Data show means  $\pm$  SDs (n = 6/time point). Data are representative of 2 independent experiments.

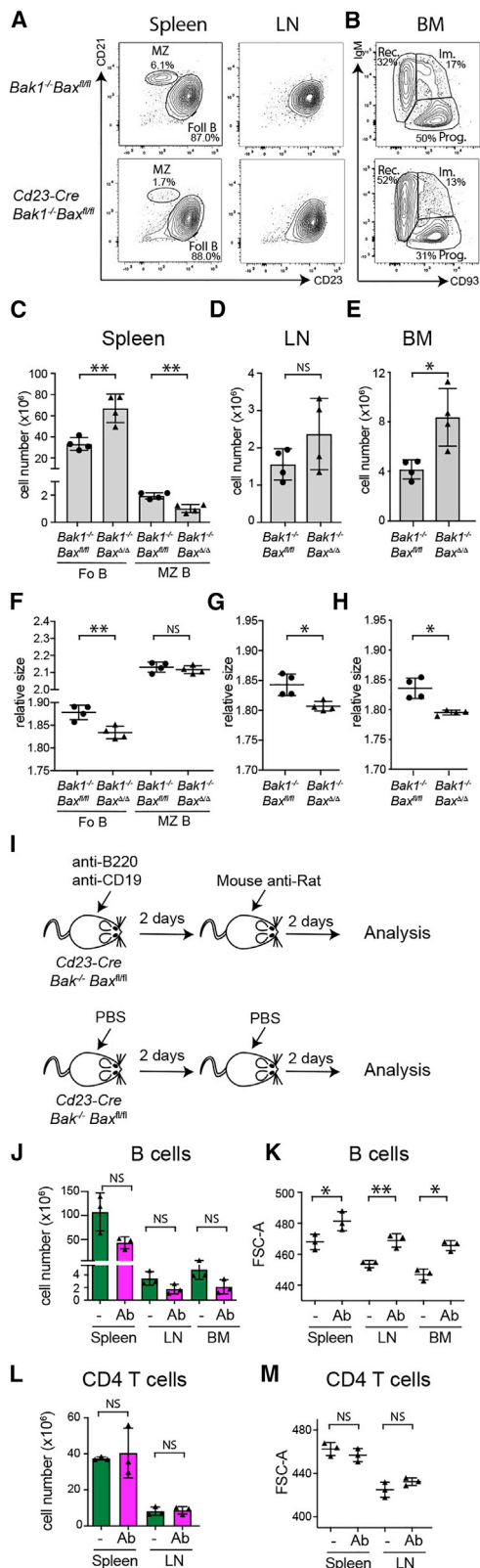


**Figure 2. Abrogation of apoptosis in mature B cells increases FoB cell numbers and decreases cell size by raising intercellular competition**

(A) Representative fluorescence-activated cell sorting (FACS) plots of CD19<sup>+</sup>CD93<sup>-</sup> mature B cells in the spleen and LNs of 10-week-old cKO mice and littermates.

(B) Representative plot of B220<sup>+</sup>CD19<sup>+</sup> B cells in the BM. Rec, recirculating FoB cells; Im, immature; and Prog, progenitor.

(C) Numbers of FoB and MZB cells in the spleen of cKO mice and littermates (n = 4).

(D) Numbers of FoB cells in LNs.

(E) Numbers of B220<sup>+</sup>CD19<sup>+</sup>CD93<sup>-</sup>IgM<sup>+</sup> mature B cells in the BM.

(F–H) Relative size of mature B cells in the spleen (F), LNs (G), and BM (H).

(I) B cell depletion in cKO mice was achieved by the injection of rat antibodies against B220 and CD19 followed by the administration of mouse anti-rat IgG antibodies 2 days later. Control mice were injected with saline.

(J) Numbers of CD93<sup>-</sup>IgM<sup>+</sup>CD23<sup>+</sup> FoB cells in the spleen, LNs, and BM.

(K) FoB cell size in the spleen, LNs, and BM.

(L) Numbers of TCRβ<sup>+</sup>CD4<sup>+</sup> T cells.

(M) CD4<sup>+</sup> T cell size in the spleen and LNs (n = 3).

Data are means ± SDs. Student's t test with \*p < 0.05, \*\*p < 0.01, and \*\*\*p < 0.001. Data are representative of 2 independent experiments.

was reduced in WT recipients, relative to those derived from control donors (Figures 3E and 3F). In contrast, they were similar in BAFF Tg recipients. Hence, reducing competition for BAFF is sufficient to restore the MZB cell population. These data indicate that the accumulation of FoB cells in cKO mice raises the intensity of competition for BAFF and thereby contracts the MZB compartment, which, in this context, is less fit than its FoB cell counterparts.

In contrast to MZB cells, splenic cKO FoB cells were increased ~2-fold in WT recipients (Figure 3G). Their individual cell size, however, was reduced (Figure 3H). Overexpression of BAFF restored their size and, importantly, it increased their number beyond those of apoptosis-sensitive controls. We then compared the size of the FoB cells receiving different levels of BAFF from their microenvironment (Figure 3I). FoB cells living in a BAFF Tg host were abnormally large, whereas *Bak1<sup>-/-</sup>Bax<sup>Δ/Δ</sup>* FoB cells deficient for the BAFF-R (encoded by the *Tnfrsf13c* gene) were highly atrophic (Figures 3I and S3). These findings establish that BAFF exerts a central non-redundant role in regulating FoB cell size *in vivo* and show that this activity is independent of its anti-apoptotic function.

Collectively, data show that the abrogation of apoptosis in mature B cells increases the size of the FoB cell compartment and thereby raises competition for BAFF. This in turn reduces FoB cell size and contracts the MZB cell compartment. Hence, our results suggest that a central role of homeostatic apoptosis in FoB cells is to restrain intercellular competition for BAFF.

### BAFF-dependent FoB cell growth *in vitro* is dependent on gene expression

Our results suggest that BAFF-R signaling is a crucial regulator of B cell size *in vivo*. We therefore aimed to better define the cellular processes underlying FoB cell growth and the anabolic activity of BAFF *in vitro*. WT cells do not lend themselves to this purpose because of their propensity to undergo apoptosis. In contrast, cKO FoB cells overcome this limitation, as they remain viable in the absence of BAFF, are remarkably resistant to cytotoxic

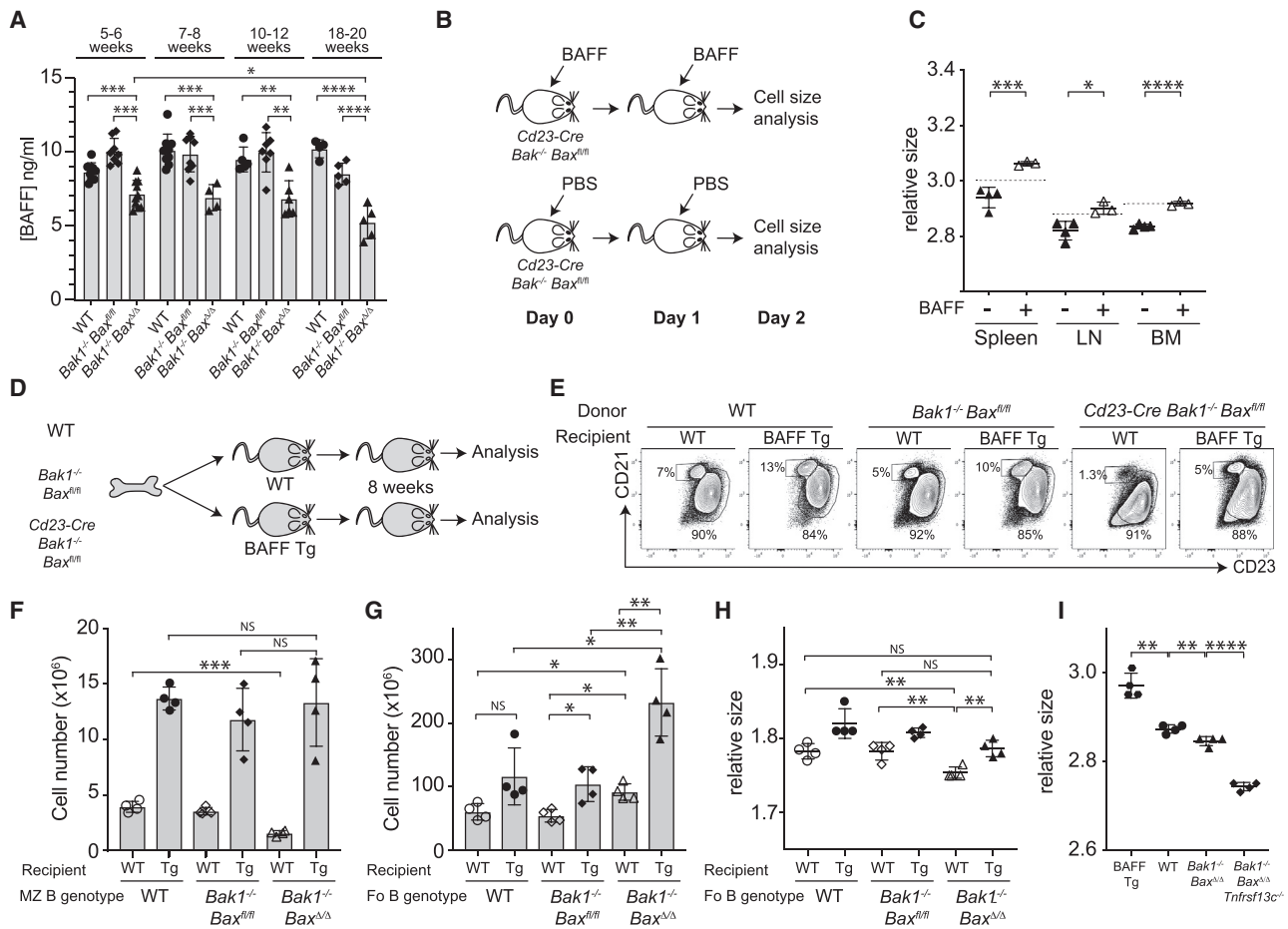


**Figure 3. BAFF is the limiting factor that restricts the numbers of mature B cells and the size of cKO FoB cells**

(A) Serum levels of BAFF in WT, *Bak1<sup>-/-</sup> Bax<sup>fl/fl</sup>*, and cKO mice of different ages.  
 (B) cKO mice were either injected with 5  $\mu$ g rBAFF or saline for 2 consecutive days. FoB cell size was measured 24 h after the last injection.  
 (C) Relative FoB cell size in spleen and LNs (n = 3–4). The dotted lines indicate the average cell size from 2 WT controls.  
 (D) BM marrow chimeras were generated by transplanting either WT, *Bak1<sup>-/-</sup> Bax<sup>fl/fl</sup>*, or cKO BM donor cells (Ly5.2<sup>+</sup>) into lethally irradiated Ly5.1 recipients. The recipients either carried a BAFF Tg expressed in radioresistant cells or were WT. Chimeras were analyzed 8 weeks post-transplant.  
 (E) Representative FACS plot of donor-derived mature B cells in the spleens of the chimeras.  
 (F and G) Numbers of splenic donor-derived MZB cells (F) and FoB cells (G).  
 (H) Relative size of donor-derived splenic FoB cells (n = 4).  
 (I) Relative size of FoB cells in the spleens of unmanipulated BAFF Tg, WT, cKO, and *Bak1<sup>-/-</sup> Bax<sup>fl/fl</sup> Cd23-Cre Tnfrsf13c<sup>-/-</sup>* mice (n = 4).  
 Data are means  $\pm$  SDs. Student's t test with \*p < 0.05; \*\*p < 0.01; \*\*\*p < 0.001; and \*\*\*\*p < 0.0001.

agents or nutrient deprivation (Figure S4), and significantly increase their size in response to treatment with BAFF (Figure 4A). We found that the absence of either dextrose (Figure 4B) or amino acids (aa) (Figure 4C) from the culture medium substantially reduced cell size and, conversely, their presence potentiated the activity of BAFF (Figures 4B and 4C). The inhibition of oxidative phosphorylation reduced B cell size and prevented the anabolic effect of BAFF (Figure 4D). These data indicate that cell growth and the activity of BAFF depend upon the presence of nutrients in the environment and on energy production. Pharmacological inhibition of translation (Figure 4E), ribosome export (Figure 4F), or transcription (Figure 4G) decreased cell size and prevented the effect of BAFF on cell growth. Interestingly, modulating transcriptional activity in FoB cells via a titra-

tion of actinomycin D resulted in a dose-dependent regulation of cell size (Figure 4H). These data support the notion that transcriptional activation induced by BAFF is essential for its activity in FoB cells.

### RNA sequencing (RNA-seq) analysis identifies transcription factors (TFs) regulating BAFF-induced cell growth

We reasoned that limiting levels of BAFF in the cKO mice may contribute to FoB cell atrophy by reducing their transcriptional capacity. Atrophy may result from the specific downregulation of TFs that activate transcription in response to BAFF. Alternatively, it may result from the activation of transcriptional repressors in response to BAFF deprivation. To identify TFs that

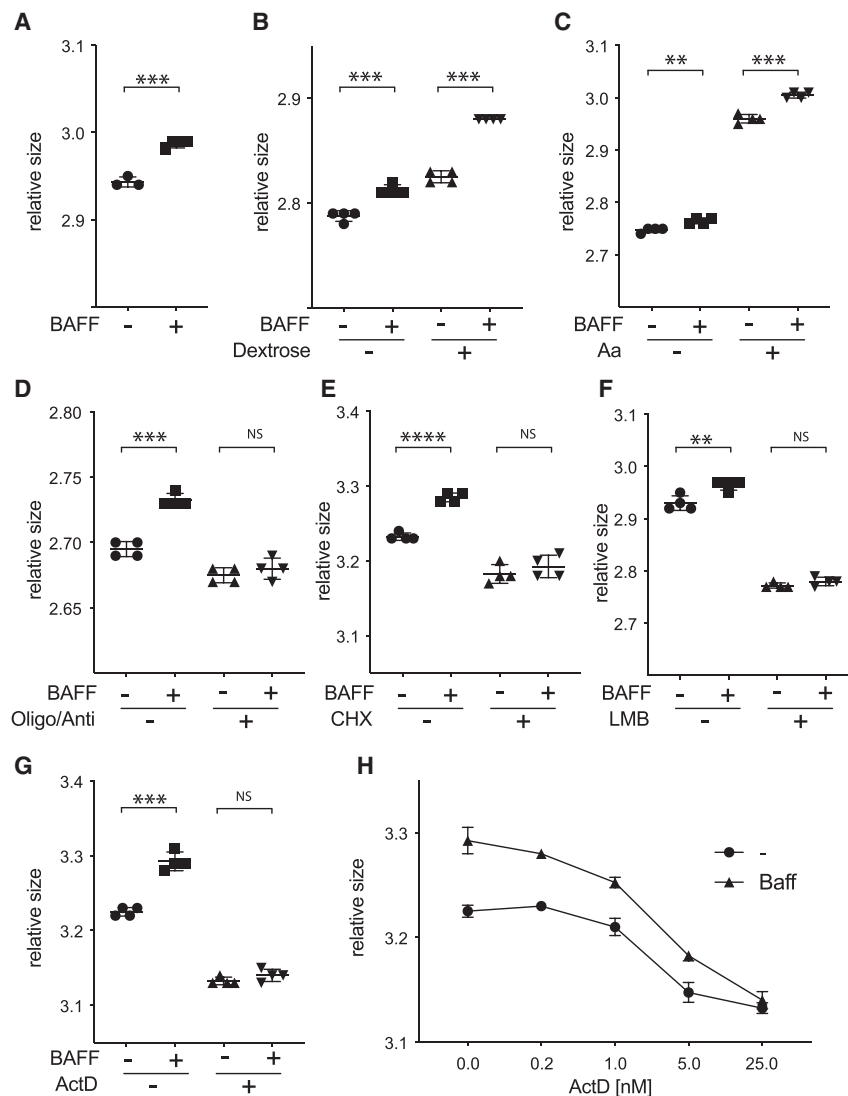


**Figure 4. BAFF-dependent FoB cell growth *in vitro* is dependent on cellular processes underpinning gene expression**

(A–G) cKO FoB cells were cultured for 48 h *in vitro* in the presence or absence of 25 ng/mL rBAFF. The effect of rBAFF on cell size was assessed either in complete DMEM (A) or in the presence or absence of the following nutrients/drugs: 5.56 mM dextrose (B), aa (C), 10  $\mu$ M oligomycin A and 4  $\mu$ M antimycin A (D), 5  $\mu$ M cyclohexamide (CHX) (E), 100 nM leptomycin B (LMB) (F), or 20 nM actinomycin D (G). (H) Titration of actinomycin D in the presence or absence of rBAFF. Each data point represents an individual measurement (technical replicate). Data are means  $\pm$  SDs. Student's t test with \* $p < 0.05$ ; \*\* $p < 0.01$  and \*\*\* $p < 0.001$ . Data are representative of at least 2 independent experiments.

enrichment analysis identified p53 gene sets (Figure 5E). To investigate whether p53 activation controls the growth of cKO FoB cells, we generated *Bak1*<sup>-/-</sup> *Bax*<sup>fl/fl</sup> *Trp53*<sup>fl/fl</sup> *CD23-Cre* mice. FoB cells in these mice were found in numbers similar to those in *Bak1*<sup>-/-</sup> *Bax*<sup>fl/fl</sup> *CD23-Cre* controls (Figure 5F), but the loss of *Trp53* trended toward increasing atrophy in the spleen and significantly aggravated it in LNs and BM (Figure 5G). These results demonstrate that p53 activation regulates FoB cell size when BAFF is limiting and represents a major brake on competition-induced atrophy.

Among the genes downregulated in cKO B cells, 18 encoded for TFs (Table S1), 8 of which were targets of the DREAM complex (Fischer et al., 2016) (Tables S1 and S2). We focused our attention on 4 TFs based on their potential in mediating B cell growth. Both *Myb* and *Spib* (Figures 5C

and S6A) have been reported to play important roles in the B cell lineage (Su et al., 1997; Thomas et al., 2005), and *Relb* and *Nfkb2* (Figures 5C and S6A) encode subunits of the dimer that plays a critical role in the non-canonical NF- $\kappa$ B pathway (Sun, 2017). We used an *in vivo* assay to test whether the downregulation of these TFs may compromise BAFF-mediated cell growth in cKO cells. BAFF Tg animals and non-Tg littermates were lethally irradiated and reconstituted with either WT BM or BM carrying a germline or conditional deletion of the gene encoding the TF of interest (Figure 5H). Eight weeks after transplantation, we assessed whether the loss of the TF precluded the accumulation of mature B cells in response to transgenic BAFF. We found that neither *Myb* nor *Spib* deficiency altered mature B cell numbers in BAFF Tg recipients (Figures S6B–S6D). In contrast, the loss of *Relb* or *Nfkb2* prevented BAFF-mediated accumulation of FoB and MZB cells in Tg recipients (Figures 5I–5K), demonstrating the *in vivo* requirement for *Relb* and *Nfkb2* in BAFF responses. These data suggest that increased

regulate BAFF-mediated cell growth, we performed RNA-seq analysis on cKO FoB cells (which live in a BAFF-low environment) and used *Bak1*<sup>-/-</sup> *Bax*<sup>fl/fl</sup> cells (which live in a BAFF-normal environment) as controls. Bioinformatic analysis identified 251 genes as downregulated in cKO B cells and 195 genes upregulated (Figure 5A). Gene set enrichment analysis revealed that transcripts encoding cell-cycle regulators were less abundant in cKO than in control FoB cells (Figure 5B). This was likely due to the upregulation of *Cdkn1a* (Figures 5C and S5), as its product, p21, stabilizes the DREAM complex, a transcriptional repressor that inhibits the expression of cell-cycle genes (Engeland, 2018). Of note, we found that 43% (109/251) of the genes downregulated in cKO B cells are DREAM complex targets (Fischer et al., 2016) (Figure 5D). *Cdkn1a* is a canonical p53 target gene (el-Deiry et al., 1993), suggesting that the deprivation of BAFF may trigger p53 activation. Consistent with this hypothesis, several p53-target genes were upregulated in cKO B cells, such as *Puma* and *Zmat3* (Figures 5C and S5), and gene set

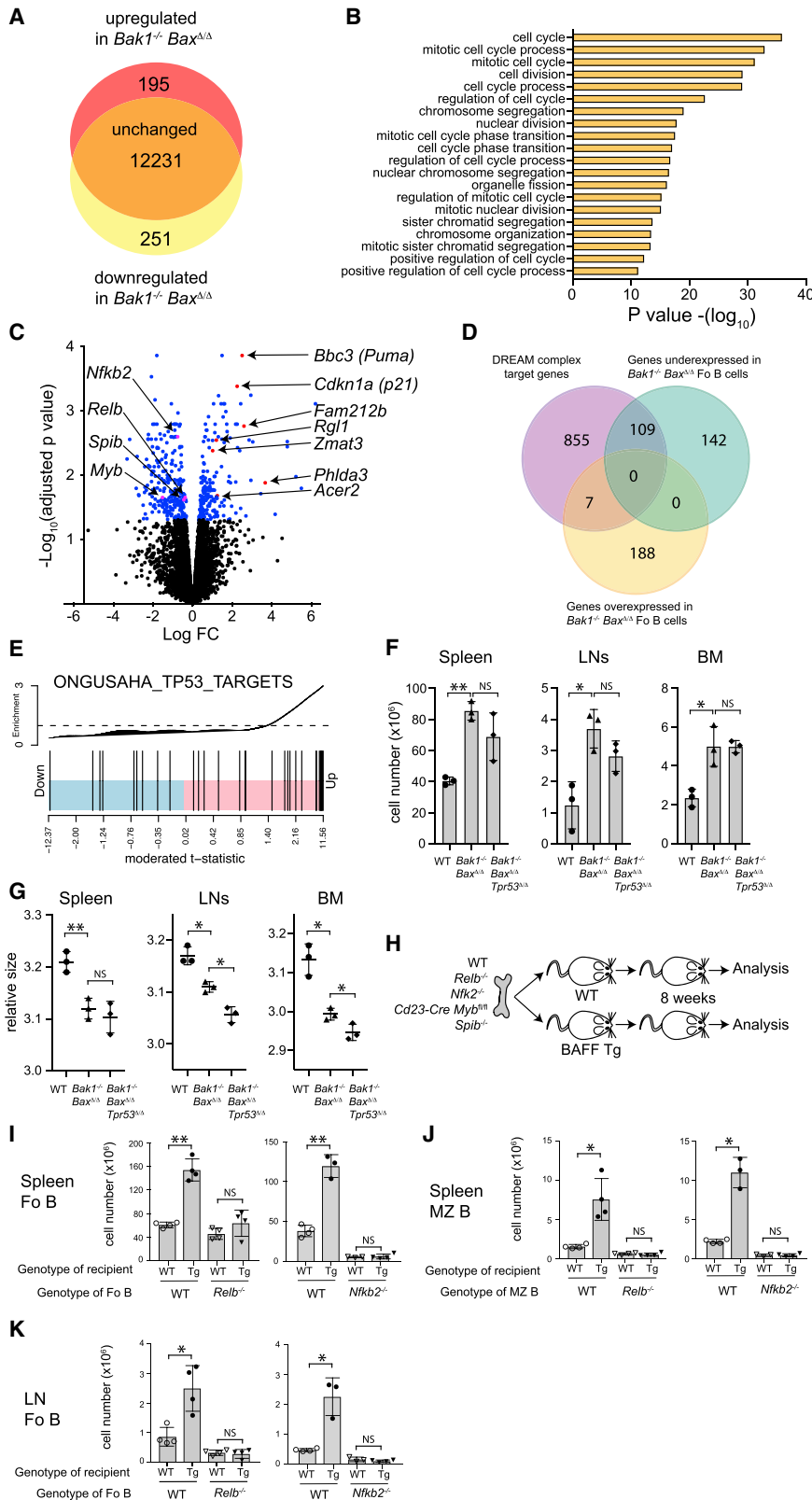


**Figure 5. RNA-seq analysis as a tool to identify TFs regulating BAFF-modulated cell growth**

(A) RNA-seq analysis identifies 251 down-regulated (including *Bax*) and 195 upregulated transcripts in cKO FoB cells compared to *Bak1<sup>-/-</sup> Bax<sup>fl/fl</sup>* cells (2% and 1.5% of detected genes, respectively).

(B) The 20 most significant gene sets identified by Gene Ontology analysis done on differentially expressed (DE) genes in cKO FoB cells.

(C) Volcano plot showing adjusted p value against fold change (FC). DE transcripts with an adjusted p < 0.05 are shown in blue.

(D) Venn diagram showing the overlap between DREAM target genes (Fischer et al., 2016) and DE genes in cKO B cells.

(E) Barcode enrichment plots showing enrichment for p53 target genes in cKO B cells.

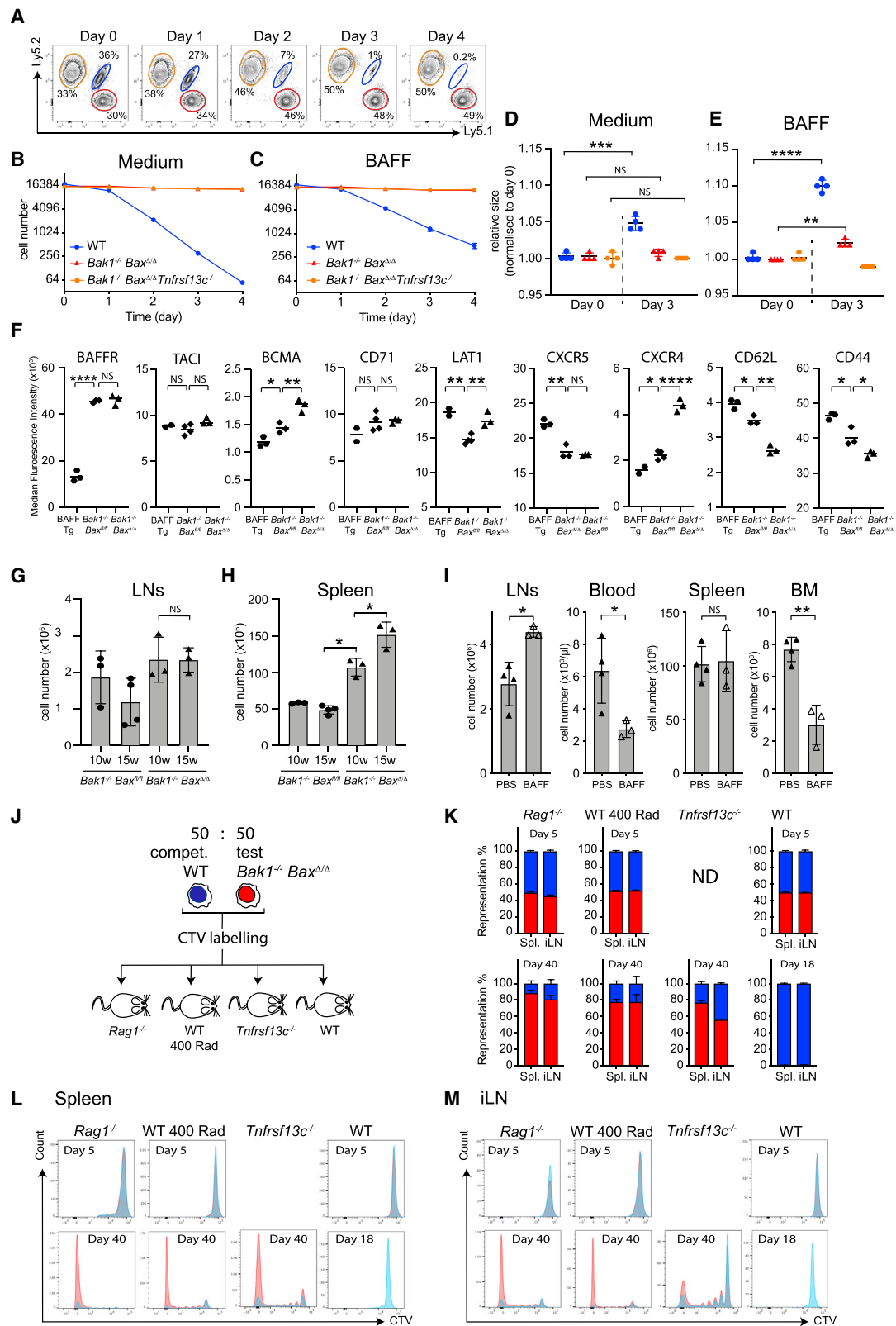
(F and G) Numbers (F) and relative size (G) of *Bak1<sup>-/-</sup> Bax<sup>ΔΔ</sup> Tpr53<sup>ΔΔ</sup>* FoB cells in the spleen, LNs, and BM (n = 3). Data show means  $\pm$  SDs.

(H) Lethally irradiated Ly5.1<sup>+</sup> BAFF Tg and non-Tg controls were reconstituted with either WT, *Relb<sup>-/-</sup>*, *Nfkb2<sup>-/-</sup>* or *Spib<sup>-/-</sup>* BM, or *Myb* cKO BM. Chimeras were analyzed 8 weeks post-transplant.

(I and J) Numbers of donor-derived splenic FoB (I) and MZB (J) cells.

(K) Numbers of donor-derived LN FoB cells (n = 3–4).

Data are means  $\pm$  SDs. Student's t test with \*p < 0.05 and \*\*p < 0.01.



(legend on next page)

competition for BAFF in cKO mice impairs FoB cell growth by reducing the activity of the non-canonical NF- $\kappa$ B pathway at the transcriptional level.

### cKO FoB cells fail to grow in nutrient-rich environment, display abnormal homing patterns, and exhibit a survival defect under competitive conditions

Growth factors can regulate cell growth by modulating the ability of cells to uptake and use nutrients (Palm and Thompson, 2017). We therefore sought to establish whether B cells receiving varying levels of BAFF signaling *in vivo* may exhibit differential growth potential *in vitro*. To this end, we purified LN FoB cells from WT, *Bak1*<sup>-/-</sup>*Bax* <sup>$\Delta/\Delta$</sup> , and *Bak1*<sup>-/-</sup>*Bax* <sup>$\Delta/\Delta$</sup> *Tnfrsf13c*<sup>-/-</sup> mice. The three B cell populations were mixed at an equal ratio and plated in complete medium in the absence or presence of recombinant BAFF (rBAFF). Each cell type carried a different allelic combination of the Ly5 congenic marker, which allowed us to track them over time (Figure 6A). Under these conditions, WT B cells cultured without rBAFF died over the course of 4 days (Figures 6B and 6C). At day 3, the remaining WT cells exhibited an increase in size even without any addition of BAFF (Figure 6D). In contrast, the numbers of viable *Bak1*<sup>-/-</sup>*Bax* <sup>$\Delta/\Delta$</sup>  and *Bak1*<sup>-/-</sup>*Bax* <sup>$\Delta/\Delta$</sup> *Tnfrsf13c*<sup>-/-</sup> B cells, and their size, remained constant throughout the experiment. As reported (Rolink et al., 2002), the addition of BAFF to the medium slowed the death rate of WT B cells (Figure 6C), suggesting that BAFF can restrain BAX/BAK-mediated apoptosis. WT cells further increased in size in response to rBAFF, whereas cKO B cells exhibited a much less pronounced increase, albeit statistically significant (Figure 6E). These results suggest that the amount of BAFF signaling received by B cells *in vivo* controls their ability to grow in nutrient-rich environments and to respond to BAFF signals *in vitro*.

To determine whether deprivation of BAFF affects the surface levels of its own receptors, nutrient receptors, adhesion molecules, or chemokine receptors, we compared the surface expression levels on FoB cells in *Cre*<sup>-</sup> control and cKO mice. We included BAFF Tg mice in our analysis to assess the effect of BAFF overexpression on the expression levels of these proteins. We found that cKO FoB cells express normal levels of BAFF-R (Figure 6F). Furthermore, the levels of the alternative BAFF receptors transmembrane activator and CAML interactor

(TACI) and B cell maturation antigen (BCMA) were unchanged and increased in cKO FoB cells, respectively (Figure 6F). These results suggest that the inability of cKO FoB cells to increase their size *in vitro* (Figures 6D and 6E) is not due to the defective expression of receptors for BAFF. Moreover, we found that expression levels of transferrin receptor (CD71) were normal in cKO cells, while those for the large neutral aa transporter LAT1 were increased (Figure 6F). While the expression levels of the chemokine receptor CXCR5 were normal in cKO FoB cells, those of CXCR4, which is crucial for the homing of recirculating FoB cells to the BM (Nie et al., 2004), were increased (Figure 6F). This suggests that heightened competition for BAFF may promote FoB cell accumulation in the BM of cKO mice (Figure 2E) by upregulating CXCR4 expression. Interestingly, the expression levels of the adhesion molecules CD44 and L-selectin (CD62L) positively correlated with the availability of BAFF (Figure 6F). Since L-selectin is instrumental for B cells to enter LNs via high endothelial venules (Tang et al., 1998), low BAFF availability may impair the entry of cKO FoB cells into LNs. Consistently, the numbers of FoB cells in the LNs of cKO mice remained constant between 10 and 15 weeks of age (Figure 6G), whereas the numbers of spleen cells increased (Figure 6H). Strikingly, the injection of rBAFF dramatically changed the distribution of FoB cells in lymphoid organs (Figure 6I). It raised the numbers of FoB cells in LNs and reduced those circulating in the blood or homing within the BM. This was specific to FoB cells, as BAFF administration did not alter the numbers or distribution of CD4 T cells (Figure S7). These findings reveal that BAFF signals regulate FoB cell extravasation toward LNs and BM homing, and indicate that this may be achieved through the modulation of CD62L and CXCR4 expression, respectively.

To address whether BAFF signals control cell competitiveness, we examined the *in vivo* fate of WT and cKO FoB cells under non-competitive and competitive conditions. cKO and WT FoB cells were purified, mixed at a 1:1 ratio, and labeled with CellTrace Violet (CTV). These cell mixtures were then adoptively transferred into recipients with either reduced or normal FoB cell compartments to assess their survival when facing endogenous competition of various intensity. *Rag1*<sup>-/-</sup>, irradiated WT, and *Tnfrsf13c*<sup>-/-</sup> mice provided a non-competitive environment while non-irradiated WT recipients offered a competitive

### Figure 6. cKO FoB cells display defective growth *in vitro*, defective competitiveness, and altered trafficking *in vivo*

Ly5.1<sup>+</sup> cKO (red) and Ly5.1<sup>+</sup> Ly5.2<sup>+</sup> WT (green) and Ly5.2<sup>+</sup> *Bak1*<sup>-/-</sup>*Bax* <sup>$\Delta/\Delta$</sup> *Tnfrsf13c*<sup>-/-</sup> (orange) B cells were isolated from LNs and mixed in equal numbers before being submitted to growth factor deprivation for 4 days.

(A) Representation of cells of each genotype over time.

(B and C) Number of viable cells of each genotype in the presence (B) or absence (C) of 25 ng/mL rBAFF.

(D and E) For each genotype, cell size was normalized for day 0 and measured after 3 days of culture in the absence (D) or presence (E) of rBAFF. Data show technical replicates with means  $\pm$  SDs. Data are representative of 2 independent experiments.

(F) Expression levels of BAFF-R, TACI, BCMA, adhesion molecules, and nutrient/chemokine receptors on FoB cells in BAFF Tg, *Bak1*<sup>-/-</sup>*Bax* <sup>$\Delta/\Delta$</sup> , and cKO mice (n = 3). Data show means. Data are representative of 3 independent experiments.

(G and H) FoB cell numbers in LNs (G) and spleens (H) of 10- and 15-week-old cKO mice and littermates (n = 3–4). Data show means  $\pm$  SDs.

(I) FoB cell numbers in LNs, blood, spleen, and BM of cKO mice injected with either PBS or BAFF (as described for Figure 3B). Data show means  $\pm$  SDs.

(J) WT competitor cells and test cKO FoB cells were mixed at a 1:1 ratio, CTV labeled, and adoptively transferred either into unmanipulated WT, *Rag1*<sup>-/-</sup>, or *Tnfrsf13c*<sup>-/-</sup> recipients or into WT recipients that had been  $\gamma$ -irradiated with 400 Rad (4 recipients/group).

(K) Representation of test and competitor FoB cells in the spleen and inguinal LNs (iLNs) of recipients 5, 18, or 40 days after transfer. Data show means  $\pm$  SDs, (n=4). N.D., not determined.

(L and M) Representative CTV profile of donor FoB cells in the spleens (L) and iLNs (M) of recipients.

Student's t test with \*p < 0.05; \*\*p < 0.01; \*\*\*p < 0.001 and \*\*\*\*p < 0.0001. Data are representative of 2 independent experiments.

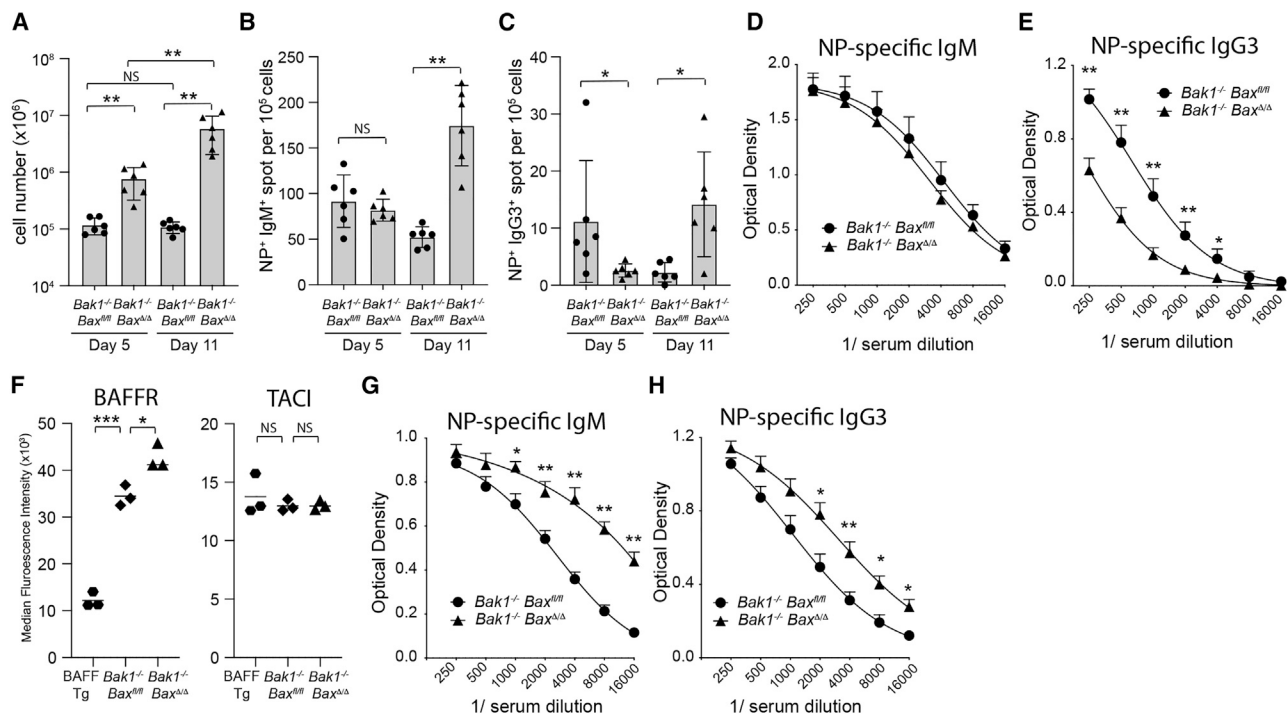


**Figure 7. Abrogation of apoptosis in mature B cells perturbs TI-antibody responses**

cKO and *Bak1*<sup>-/-</sup> *Bax*<sup>fl/fl</sup> littermates were immunized intraperitoneally (i.p.) with NP-Ficoll and analyzed 5 and 11 days later. (A) Numbers of splenic B220<sup>+</sup>CD138<sup>+</sup> plasmablasts determined by flow cytometry 5 and 11 days post-immunization. (B and C) ELISpot analysis of NP<sup>+</sup>IgM<sup>+</sup> (B) and NP<sup>+</sup>IgG3<sup>+</sup> (C) splenic antibody-secreting cells 5 and 11 days post-immunization. (D and E) ELISA analysis of NP-specific IgM (D) and IgG3 (E) serum antibody 5 days post-immunization. Data show means ± SEMs (n = 6). Mann-Whitney nonparametric, 2-tailed test with \*p < 0.05 and \*\*p < 0.01. Data are representative of 2 independent experiments. (F) Expression levels of BAFF-R and TACI on MZ B cells in BAFF Tg, *Bak1*<sup>-/-</sup> *Bax*<sup>fl/fl</sup>, and cKO mice (n = 3). Student's t test with \*p < 0.05 and \*\*\*p < 0.001. Data are representative of 3 independent experiments. (G and H) ELISA analysis of NP-specific IgM (G) and IgG3 (H) serum antibody 11 days post-immunization (n = 6). Data show means ± SEMs. Mann-Whitney nonparametric, 2-tailed test with \*p < 0.05 and \*\*p < 0.01.

environment (Figure 6J). Five days after transfusion, cKO FoB cells were present at the same frequency as WT FoB cells in the spleen and inguinal LNs (Figure 6K), and neither cell type had undergone cell division (Figures 6L and 6M). After 40 days in a non-competitive environment, cKO FoB cells were overrepresented compared to WT control FoB cells (Figure 6K). As expected (Cabatingan et al., 2002), their CTV profile showed that these cKO FoB cells were in most cases the product of several rounds of division (Figures 6L and 6M). This demonstrates that cKO FoB cells can survive for extended periods of time under non-competitive conditions and that resistance to apoptosis confers a substantial survival advantage over their co-transplanted WT counterparts during lymphopenia-induced proliferation. In striking contrast, 18 days after transfer into unmanipulated WT recipients (competitive condition), cKO FoB cells were completely absent, whereas their WT competitors were still present in the recipients' spleens and LNs without having undergone proliferation (Figures 6K–6M). These results demonstrate that cKO FoB cells have a profound survival defect under normal competitive conditions.

These findings indicate that by restraining competition for BAFF, apoptosis modulates fundamental aspects of FoB cell

physiology, such as cell growth in response to nutrients and BAFF, migration, and competitiveness.

### Thymus-independent (TI) antibody responses are perturbed in cKO animals

We next investigated whether the disruption of apoptosis may compromise mature B cell function. We immunized cKO mice and littermate controls with 4-hydroxy-3-nitrophenylacetic (NP)-Ficoll to elicit a TI antibody response. After 5 days, the total numbers of plasmablasts were increased in the spleen (Figure 7A), suggesting that the disruption of apoptosis does not hinder B cell activation. However, while the numbers of NP-specific cells secreting IgM were normal at this time point (Figure 7B), the numbers of cells producing IgG3 were lower than in control mice (Figure 7C). These results were mirrored in the serum of cKO mice, where titers of NP-specific IgM and IgG3 were normal and reduced, respectively (Figure 7D and 7E), suggesting that Ig class switch recombination (CSR) was delayed or impaired in cKO mice. Because BAFF can support CSR by signaling through both BAFF-R and TACI (Castigli et al., 2005), we investigated the levels of these receptors by flow cytometry. They were normal in cKO FoB cells (Figure 6F) and BAFF-R levels were increased in

cKO MZB cells while those of TAC1 were unchanged (Figure 7F). These results show that the disruption of apoptosis in mature B cells compromises the generation of antigen-specific IgG3 antibodies in the early phase of TI humoral immune response, possibly by putting a brake on BAFF/BAFF-R signaling-supported Ig CSR.

We next assessed whether abrogation of apoptosis only delayed the induction of the humoral immune response against NP-FicolI or whether it continued to undermine it/inhibit the response over time. To this end, we analyzed cKO and control mice 11 days after immunization. While the numbers of plasma blasts in control mice did not significantly change between 5 and 11 days post-immunization, those in cKO mice increased during this time frame (Figure 7A). Furthermore, 11 days after immunization, the numbers of NP-specific cells secreting IgM and IgG3 in cKO mice both exceeded those of control littermates (Figures 7B and 7C) and the antibody titers in the serum were accordingly increased (Figures 7G and 7H). These results suggest that in WT mice, apoptosis limits the production of antigen-specific antibodies during the later phase of TI humoral responses by constraining the numbers of antibody-secreting cells.

These findings suggest that abrogation of apoptosis substantially perturbs TI humoral responses. Five days after antigenic challenge, it limits the generation of antigen-specific IgG3<sup>+</sup> plasma cells and serum IgG3<sup>+</sup> antibodies, whereas in contrast, 11 days after immunization, it increases the amplitude of the antigen-specific humoral response.

## DISCUSSION

We found that under homeostatic conditions, the turnover of distinct subsets of mature B cells is differentially regulated by apoptosis. FoB cells reaching the end of their lifespan die via apoptosis, but this is not the case for MZB cells. We demonstrate that the disruption of apoptosis leads to the accumulation of FoB cells in lymphoid organs, which in turn increases intercellular competition for BAFF. This has dramatic consequences for all mature B cell subsets, contracting the MZB cell compartment and altering fundamental aspects of FoB cell physiology. Hence, our results support a model whereby competition for cell-type-specific growth factors produced in limiting quantities underpins tissue homeostasis (Raff, 1992) and illustrate how changes in competition intensity affect lymphoid homeostasis (Freitas and Rocha, 2000).

The apoptosis pathway is operative in MZB cells as seen by the fact that WT cells undergo apoptosis in response to ABT-737 and growth factor deprivation *in vitro* and that inducible *Mcl-1* deletion depletes MZB cells (Vikström et al., 2016). However, our BrdU labeling experiments demonstrate that apoptosis does not constrain the MZB cell lifespan in normal mice *in vivo*. Thus, apoptosis is dispensable for MZB cell homeostasis, an emerging theme in studies of other mammalian tissues (Ke et al., 2018; Lindsten et al., 2000; Lindsten and Thompson, 2006). It is increasingly evident that the role played by apoptosis in the homeostatic turnover of a given cell population cannot be inferred from the apoptotic death of these cells *in vitro*, but requires the evaluation of their lifespan at steady state *in vivo*.

Our data imply that MZB cell turnover is controlled by mechanisms other than the intrinsic apoptotic pathway. Necroptosis and death receptor-induced apoptosis are unlikely to be implicated because B lymphoid homeostasis is normal in mice in which these pathways are abrogated (Alvarez-Diaz et al., 2016). While MZB cells can undergo ferroptosis in response to lipid peroxidation (Muri et al., 2019), whether it is engaged under homeostatic conditions is unknown. Conceivably, the turnover of MZB cells may occur through the concerted activation of multiple genetically programmed cell death pathways (Bedoui et al., 2020). It could also be affected independent of genetically programmed pathways, perhaps akin to the disposal of aged red blood cells by macrophages (de Back et al., 2014).

While BAFF-R signaling is instrumental for the survival of FoB and MZB cells *in vivo* (Rauch et al., 2009), it likely controls the viability of these cells through different pathways. Resistance to apoptosis allows the progressive enlargement of the FoB cell population, despite low BAFF availability in cKO mice, whereas in contrast, it fails to protect the MZB cell population, which contracts under the same conditions. The number of cKO FoB cells that develop in BAFF Tg recipients exceeds those of apoptosis-sensitive cells, yet the same is not true for cKO MZB cells. Furthermore, abrogation of apoptosis *in vivo* can partially substitute for BAFF-R activity in FoB cells, but fails to do so in MZB cells (Tardivel et al., 2004). These findings indicate that BAFF-R signaling promotes survival in FoB cells by antagonizing apoptosis, while in MZB cells this is achieved by a non-apoptotic, as-yet-unknown pathway. They further suggest that resistance to apoptosis renders FoB cells but not MZB cells less dependent on BAFF signals for survival, which may explain why it extends the *in vivo* lifespan of the former but not of the latter.

In FoB cells, BAFF is thought to block apoptosis by modulating the expression of key apoptotic regulators (Craxton et al., 2005; Do et al., 2000; Hsu et al., 2002; Jacque et al., 2015; Woodland et al., 2008). We show that BAFF deprivation *in vivo* activates p53 and triggers the upregulation of *Puma*, a major pro-apoptotic p53 target (Nakano and Vousden, 2001; Villunger et al., 2003). Hence, our results suggest that WT FoB cells that have failed to receive BAFF signals beyond a critical threshold may undergo apoptosis as a result of p53 activation.

In FoB cells that are normally sensitive to apoptosis, interference with BAFF-R signaling rapidly triggers cell death, which precludes a comprehensive understanding of the role of BAFF in the physiology of these cells. The disruption of apoptosis in cKO FoB cells overcomes this limitation and offers an opportunity to identify novel facets of FoB cell biology that are regulated by BAFF.

We show that the abrogation of apoptosis in mature B cells leads to the enlargement of the FoB cell compartment in the spleen and BM, thereby raising the intercellular competition for BAFF, which in turn compromises the growth of FoB cells. Decreasing competition for BAFF is sufficient to restore FoB cell size and to further increase their numbers. This demonstrates that the limited BAFF availability (Mackay et al., 1999; Wilhelmson et al., 2018) enforces competition among mature B cells and naturally constrains FoB cell size and number. Our results further suggest that BAFF-R signaling may further affect FoB cell growth by

modulating the potential of the cells to grow in nutrient-rich environments. While our results are consistent with the role of growth factors in regulating nutrient uptake (Lum et al., 2005; Palm and Thompson, 2017), we did not find evidence that BAFF deprivation decreased the expression of nutrient receptors as observed *in vitro* for other growth factors (Edinger and Thompson, 2002; Rathmell et al., 2003). We found that cKO FoB cells are prematurely cleared under normal competitive conditions *in vivo* despite their profound resistance to apoptosis. Cells with decreased gene expression are known to be efficiently eliminated at the expense of normal competitors (Clavería et al., 2013; Morata and Ripoll, 1975; Oliver et al., 2004). By regulating gene expression and cell growth, BAFF signals may therefore regulate B cell competitiveness. Hence, autocrine provision of BAFF in malignancies could undermine the tumor suppressor function that is normally exerted by cell competition *in vivo* (Martins et al., 2014). The understanding that BAFF availability affects cell growth and competitiveness *in vivo* may be relevant for elucidating the relationship between BAFF overexpression and B cell malignancies in humans (He et al., 2004; Kern et al., 2004; Moreaux et al., 2004) and mice (Batten et al., 2004).

Our findings reveal an underappreciated role for BAFF in regulating FoB cell homing and trafficking. We show that the administration of rBAFF is sufficient to restore the ability of blood-borne FoB cells to enter peripheral LNs in cKO mice. Coincidentally, the levels of L-selectin, an adhesion molecule essential for LN extravasation (Tang et al., 1998) reflect BAFF availability. In contrast, CXCR4 expression on FoB cells is inversely correlated with BAFF availability, which may drive the accumulation of cKO cells in the BM (Brenner et al., 2004). Raising BAFF levels in cKO mice releases FoB cells from this niche. Collectively, our findings show that BAFF-R signaling controls FoB cell migration and suggest that it may do so by modulating the expression of critical regulators of cell trafficking.

We show that transcription is necessary for BAFF-driven cell growth *in vitro*, suggesting that BAFF-induced transcription is instrumental to sustain B cell growth. Because cKO FoB cells survive under reduced BAFF availability, these cells can be used as an *in vivo* platform to identify transcriptional programs that regulate BAFF-driven cell growth. Our analysis identified that transcripts encoding *Nfkb2* and *Relb*, the two subunits of the critical effector of the non-canonical NF- $\kappa$ B pathway, were reduced in cKO B cells, suggesting that they may act downstream of BAFF-R. Constitutive NF- $\kappa$ B activation restores the survival and numbers of mature B cells in BAFF and BAFFR KO mice (Gardam et al., 2008; Gardam et al., 2011; Sasaki et al., 2006). This indicates that the NF- $\kappa$ B pathway is the main, if not the sole, transcriptional program that is critical for the cellular responses to BAFF. Accordingly, our BM chimera experiments demonstrate that both *Nfkb2* and *Relb* are indispensable for the responsiveness of mature B cells to BAFF. It is known that BAFF supports *Nfkb2* transcription (De Silva et al., 2016) and that *Relb* promotes its own transcription in a feedforward process (Bren et al., 2001). Hence, the decreased availability of BAFF may directly cause the combined downregulation of *Nfkb2* and *Relb* in cKO FoB cells. This may in turn severely compromise the transcription of NF- $\kappa$ B target genes as the co-deletion of *Nfkb2* and *Relb* is more detrimental to mature B cells

than the loss of either alone (De Silva et al., 2016). Hence, our findings support the notion that BAFF deprivation causes FoB cell atrophy by dampening the non-canonical NF- $\kappa$ B pathway at the transcriptional level.

Our results further suggest that BAFF deprivation causes p53 activation. Supporting the idea that the effector mechanisms of p53 are context dependent (Kastenhuber and Lowe, 2017), we show that p53 plays a non-redundant role in cKO FoB cell growth and restrains atrophy. Whether this protective response depends on macro-autophagy (Feng et al., 2005; Tasdemir et al., 2008) or whether it drives other p53-driven processes remains to be established.

In conclusion, we show that apoptosis regulates the FoB cell lifespan, but it does not control the lifespan of MZB cells. We further demonstrate that the blockade of apoptosis in mature B cells increases FoB cell numbers and thereby raises intercellular competition for BAFF. This in turn reduces the size of the MZB cell compartment, perturbs TI-antibody responses, and profoundly affects the physiology of FoB cells by altering their migration and by undermining their size, as well as their ability to grow and to compete. Hence, our results suggest that the essential role of apoptosis is to limit the stringency of intercellular competition for BAFF among mature B cells.

## STAR★METHODS

Detailed methods are provided in the online version of this paper and include the following:

- KEY RESOURCES TABLE
- RESOURCE AVAILABILITY
  - Lead contact
  - Materials availability
  - Data and code availability
- EXPERIMENTAL MODEL AND SUBJECT DETAILS
  - Mice
  - Animal experiments
- METHOD DETAILS
  - Flow cytometry
  - BrdU labeling in mixed BM chimeric mice
  - *In vitro* assays
  - Deletion of the floxed Bax allele
  - Transcriptome analyses
  - Bioinformatics analysis
  - ELISA
  - ELISpot
  - Immunofluorescence
- QUANTIFICATION AND STATISTICAL ANALYSIS

## SUPPLEMENTAL INFORMATION

Supplemental information can be found online at <https://doi.org/10.1016/j.celrep.2021.109430>.

## ACKNOWLEDGMENTS

We thank S. Nutt and S. Willis for *Spib*<sup>-/-</sup> mice, F. Mackay for BAFF Tg and *Tnfrsf13c*<sup>-/-</sup> mice, and U. Siebenlist for *Nfkb2*<sup>-/-</sup> mice. We thank the WEHI Bioservices staff for mouse work and are grateful to T. Saunders for critically

reviewing the manuscript. This work was supported by an Australian Federal Government Postgraduate Award (to K.M.); Project Grants (1077750 and 1106471), Program Grants (1016647, 1113577, and 101671), and Fellowships (1063008 to B.T.K., 1020363 to A.S., and 1161352 to K.M.); Bellberry-Viertel Senior Medical Research Fellowship (to K.L.G.-J.); an Independent Research Institutes Infrastructure Support Scheme Grant (361646) from the Australian National Health and Medical Research Council; the Australian Cancer Research Fund; a SCOR grant (7001-13) from the Leukemia and Lymphoma Society (US); and a Victorian State Government Operational Infrastructure Support Grant.

#### AUTHOR CONTRIBUTIONS

S.C. and B.T.K. conceptualized the study and designed the experiments. S.C., K.M., L.K., M.T., R.M.L., and A.L. performed the experiments. S.C. and L.K. analyzed the data. C.W.L. and M.E.R. performed the bioinformatics analysis. B.T.K. acquired the funding. S.C. wrote the original draft. S.C., K.M., A.S., K.L.G.-J., and B.T.K. reviewed and edited the manuscript.

#### DECLARATION OF INTERESTS

The authors declare no competing interests.

Received: December 14, 2020

Revised: April 13, 2021

Accepted: June 30, 2021

Published: July 20, 2021

#### SUPPORTING CITATIONS

The following references appear in the supplemental information: Allman et al. (2001).

#### REFERENCES

Allman, D., Lindsley, R.C., DeMuth, W., Rudd, K., Shinton, S.A., and Hardy, R.R. (2001). Resolution of three nonproliferative immature splenic B cell subsets reveals multiple selection points during peripheral B cell maturation. *J. Immunol.* *167*, 6834–6840.

Almaden, J.V., Tsui, R., Liu, Y.C., Birnbaum, H., Shokhirev, M.N., Ngo, K.A., Davis-Turak, J.C., Otero, D., Basak, S., Rickert, R.C., and Hoffmann, A. (2014). A pathway switch directs BAFF signaling to distinct NF- $\kappa$ B transcription factors in maturing and proliferating B cells. *Cell Rep.* *9*, 2098–2111.

Alvarez-Diaz, S., Dillon, C.P., Lalaoui, N., Tanzer, M.C., Rodriguez, D.A., Lin, A., Lebois, M., Hakem, R., Josefsson, E.C., O'Reilly, L.A., et al. (2016). The Pseudokinase MLKL and the Kinase RIPK3 Have Distinct Roles in Autoimmune Disease Caused by Loss of Death-Receptor-Induced Apoptosis. *Immunity* *45*, 513–526.

Batten, M., Fletcher, C., Ng, L.G., Groom, J., Wheway, J., Laâbi, Y., Xin, X., Schneider, P., Tschopp, J., Mackay, C.R., and Mackay, F. (2004). TNF deficiency fails to protect BAFF transgenic mice against autoimmunity and reveals a predisposition to B cell lymphoma. *J. Immunol.* *172*, 812–822.

Bedoui, S., Herold, M.J., and Strasser, A. (2020). Emerging connectivity of programmed cell death pathways and its physiological implications. *Nat. Rev. Mol. Cell Biol.* *21*, 678–695.

Bren, G.D., Solan, N.J., Miyoshi, H., Pennington, K.N., Pobst, L.J., and Paya, C.V. (2001). Transcription of the RelB gene is regulated by NF- $\kappa$ B. *Oncogene* *20*, 7722–7733.

Brenner, S., Whiting-Theobald, N., Kawai, T., Linton, G.F., Rudikoff, A.G., Choi, U., Ryser, M.F., Murphy, P.M., Sechler, J.M., and Malech, H.L. (2004). CXCR4-transgene expression significantly improves marrow engraftment of cultured hematopoietic stem cells. *Stem Cells* *22*, 1128–1133.

Cabatingan, M.S., Schmidt, M.R., Sen, R., and Woodland, R.T. (2002). Naive B lymphocytes undergo homeostatic proliferation in response to B cell deficit. *J. Immunol.* *169*, 6795–6805.

Castigli, E., Wilson, S.A., Scott, S., Dedeoglu, F., Xu, S., Lam, K.P., Bram, R.J., Jabara, H., and Geha, R.S. (2005). TACI and BAFF-R mediate isotype switching in B cells. *J. Exp. Med.* *201*, 35–39.

Claudio, E., Brown, K., Park, S., Wang, H., and Siebenlist, U. (2002). BAFF-induced NEMO-independent processing of NF- $\kappa$ B2 in maturing B cells. *Nat. Immunol.* *3*, 958–965.

Claveria, C., Giovinazzo, G., Sierra, R., and Torres, M. (2013). Myc-driven endogenous cell competition in the early mammalian embryo. *Nature* *500*, 39–44.

Craxton, A., Draves, K.E., Gruppi, A., and Clark, E.A. (2005). BAFF regulates B cell survival by downregulating the BH3-only family member Bim via the ERK pathway. *J. Exp. Med.* *202*, 1363–1374.

Cremasco, V., Woodruff, M.C., Onder, L., Cupovic, J., Nieves-Bonilla, J.M., Schildberg, F.A., Chang, J., Cremasco, F., Harvey, C.J., Wucherpfennig, K., et al. (2014). B cell homeostasis and follicle confines are governed by fibroblastic reticular cells. *Nat. Immunol.* *15*, 973–981.

Crowley, J.E., Scholz, J.L., Quinn, W.J., 3rd, Stadanick, J.E., Trembl, J.F., Trembl, L.S., Hao, Y., Goenka, R., O'Neill, P.J., Matthews, A.H., et al. (2008). Homeostatic control of B lymphocyte subsets. *Immunol. Res.* *42*, 75–83.

de Back, D.Z., Kostova, E.B., van Kraaij, M., van den Berg, T.K., and van Bruggen, R. (2014). Of macrophages and red blood cells; a complex love story. *Front. Physiol.* *5*, 9.

De Silva, N.S., Silva, K., Anderson, M.M., Bhagat, G., and Klein, U. (2016). Impairment of Mature B Cell Maintenance upon Combined Deletion of the Alternative NF- $\kappa$ B Transcription Factors RELB and NF- $\kappa$ B2 in B Cells. *J. Immunol.* *196*, 2591–2601.

Delbridge, A.R., Grabow, S., Strasser, A., and Vaux, D.L. (2016). Thirty years of BCL-2: translating cell death discoveries into novel cancer therapies. *Nat. Rev. Cancer* *16*, 99–109.

Do, R.K., Hatada, E., Lee, H., Tourigny, M.R., Hilbert, D., and Chen-Kiang, S. (2000). Attenuation of apoptosis underlies B lymphocyte stimulator enhancement of humoral immune response. *J. Exp. Med.* *192*, 953–964.

Edinger, A.L., and Thompson, C.B. (2002). Akt maintains cell size and survival by increasing mTOR-dependent nutrient uptake. *Mol. Biol. Cell* *13*, 2276–2288.

el-Deiry, W.S., Tokino, T., Velculescu, V.E., Levy, D.B., Parsons, R., Trent, J.M., Lin, D., Mercer, W.E., Kinzler, K.W., and Vogelstein, B. (1993). WAF1, a potential mediator of p53 tumor suppression. *Cell* *75*, 817–825.

Emambokus, N., Vegiopoulos, A., Harman, B., Jenkinson, E., Anderson, G., and Frampton, J. (2003). Progression through key stages of haemopoiesis is dependent on distinct threshold levels of c-Myb. *EMBO J.* *22*, 4478–4488.

Enders, A., Bouillet, P., Puthalath, H., Xu, Y., Tarlinton, D.M., and Strasser, A. (2003). Loss of the pro-apoptotic BH3-only Bcl-2 family member Bim inhibits BCR stimulation-induced apoptosis and deletion of autoreactive B cells. *J. Exp. Med.* *198*, 1119–1126.

Engeland, K. (2018). Cell cycle arrest through indirect transcriptional repression by p53: I have a DREAM. *Cell Death Differ.* *25*, 114–132.

Enzler, T., Bonizzi, G., Silverman, G.J., Otero, D.C., Widhopf, G.F., Anzelon-Mills, A., Rickert, R.C., and Karin, M. (2006). Alternative and classical NF- $\kappa$ B signaling retain autoreactive B cells in the splenic marginal zone and result in lupus-like disease. *Immunity* *25*, 403–415.

Feng, Z., Zhang, H., Levine, A.J., and Jin, S. (2005). The coordinate regulation of the p53 and mTOR pathways in cells. *Proc. Natl. Acad. Sci. USA* *102*, 8204–8209.

Fischer, M., Grossmann, P., Padi, M., and DeCaprio, J.A. (2016). Integration of TP53, DREAM, MMB-FOXO1 and RB-E2F target gene analyses identifies cell cycle gene regulatory networks. *Nucleic Acids Res.* *44*, 6070–6086.

Förster, I., and Rajewsky, K. (1990). The bulk of the peripheral B-cell pool in mice is stable and not rapidly renewed from the bone marrow. *Proc. Natl. Acad. Sci. USA* *87*, 4781–4784.

Acad. Sci. USA 87, 4781–4784.

Franzoso, G., Carlson, L., Poljak, L., Shores, E.W., Epstein, S., Leonardi, A., Grinberg, A., Tran, T., Scharton-Kersten, T., Anver, M., et al. (1998). Mice deficient in nuclear factor (NF)- $\kappa$ B/p52 present with defects in humoral

- responses, germinal center reactions, and splenic microarchitecture. *J. Exp. Med.* **187**, 147–159.
- Freitas, A.A., and Rocha, B. (2000). Population biology of lymphocytes: the flight for survival. *Annu. Rev. Immunol.* **18**, 83–111.
- Gardam, S., Sierro, F., Basten, A., Mackay, F., and Brink, R. (2008). TRAF2 and TRAF3 signal adapters act cooperatively to control the maturation and survival signals delivered to B cells by the BAFF receptor. *Immunity* **28**, 391–401.
- Gardam, S., Turner, V.M., Anderton, H., Limaye, S., Basten, A., Koentgen, F., Vaux, D.L., Silke, J., and Brink, R. (2011). Deletion of cIAP1 and cIAP2 in murine B lymphocytes constitutively activates cell survival pathways and inactivates the germinal center response. *Blood* **117**, 4041–4051.
- Giam, M., Huang, D.C., and Bouillet, P. (2008). BH3-only proteins and their roles in programmed cell death. *Oncogene* **27** (Suppl 1), S128–S136.
- Gorelik, L., Gilbride, K., Dobles, M., Kalled, S.L., Zandman, D., and Scott, M.L. (2003). Normal B cell homeostasis requires B cell activation factor production by radiation-resistant cells. *J. Exp. Med.* **198**, 937–945.
- Gorelik, L., Cutler, A.H., Thill, G., Miklasz, S.D., Shea, D.E., Ambrose, C., Bixler, S.A., Su, L., Scott, M.L., and Kalled, S.L. (2004). Cutting edge: BAFF regulates CD21/35 and CD23 expression independent of its B cell survival function. *J. Immunol.* **172**, 762–766.
- Gross, A., and Katz, S.G. (2017). Non-apoptotic functions of BCL-2 family proteins. *Cell Death Differ.* **24**, 1348–1358.
- Hao, Z., and Rajewsky, K. (2001). Homeostasis of peripheral B cells in the absence of B cell influx from the bone marrow. *J. Exp. Med.* **194**, 1151–1164.
- Harless, S.M., Lentz, V.M., Sah, A.P., Hsu, B.L., Clise-Dwyer, K., Hilbert, D.M., Hayes, C.E., and Cancro, M.P. (2001). Competition for BlyS-mediated signaling through Bcmd/BR3 regulates peripheral B lymphocyte numbers. *Curr. Biol.* **11**, 1986–1989.
- He, B., Chadburn, A., Jou, E., Schattner, E.J., Knowles, D.M., and Cerutti, A. (2004). Lymphoma B cells evade apoptosis through the TNF family members BAFF/BlyS and APRIL. *J. Immunol.* **172**, 3268–3279.
- Hsu, B.L., Harless, S.M., Lindsley, R.C., Hilbert, D.M., and Cancro, M.P. (2002). Cutting edge: BlyS enables survival of transitional and mature B cells through distinct mediators. *J. Immunol.* **168**, 5993–5996.
- Jacque, E., Schweighoffer, E., Tybulewicz, V.L., and Ley, S.C. (2015). BAFF activation of the ERK5 MAP kinase pathway regulates B cell survival. *J. Exp. Med.* **212**, 883–892.
- Jonkers, J., Meuwissen, R., van der Gulden, H., Peterse, H., van der Valk, M., and Berns, A. (2001). Synergistic tumor suppressor activity of BRCA2 and p53 in a conditional mouse model for breast cancer. *Nat. Genet.* **29**, 418–425.
- Kastenhuber, E.R., and Lowe, S.W. (2017). Putting p53 in Context. *Cell* **170**, 1062–1078.
- Kayagaki, N., Yan, M., Seshasayee, D., Wang, H., Lee, W., French, D.M., Grewal, I.S., Cochran, A.G., Gordon, N.C., Yin, J., et al. (2002). BAFF/BlyS receptor 3 binds the B cell survival factor BAFF ligand through a discrete surface loop and promotes processing of NF- $\kappa$ B2. *Immunity* **17**, 515–524.
- Ke, F.F.S., Vanyai, H.K., Cowan, A.D., Delbridge, A.R.D., Whitehead, L., Grabow, S., Czabotar, P.E., Voss, A.K., and Strasser, A. (2018). Embryogenesis and Adult Life in the Absence of Intrinsic Apoptosis Effectors BAX, BAK, and BOK. *Cell* **173**, 1217–1230.e17.
- Kern, C., Cornuel, J.F., Billard, C., Tang, R., Rouillard, D., Stenou, V., Defrance, T., Ajchenbaum-Cymbalista, F., Simonin, P.Y., Feldblum, S., and Kolb, J.P. (2004). Involvement of BAFF and APRIL in the resistance to apoptosis of B-CLL through an autocrine pathway. *Blood* **103**, 679–688.
- Kwon, K., Hutter, C., Sun, Q., Bilic, I., Cobaleda, C., Malin, S., and Busslinger, M. (2008). Instructive role of the transcription factor E2A in early B lymphopoiesis and germinal center B cell development. *Immunity* **28**, 751–762.
- Lam, K.P., Kühn, R., and Rajewsky, K. (1997). In vivo ablation of surface immunoglobulin on mature B cells by inducible gene targeting results in rapid cell death. *Cell* **90**, 1073–1083.
- Law, C.W., Chen, Y., Shi, W., and Smyth, G.K. (2014). voom: precision weights unlock linear model analysis tools for RNA-seq read counts. *Genome Biol.* **15**, R29.
- Lee, E.F., Grabow, S., Chappaz, S., Dewson, G., Hockings, C., Kluck, R.M., Debrincat, M.A., Gray, D.H., Witkowski, M.T., Evangelista, M., et al. (2016). Physiological restraint of Bak by Bcl-xL is essential for cell survival. *Genes Dev.* **30**, 1240–1250.
- Liao, Y., Smyth, G.K., and Shi, W. (2013). The Subread aligner: fast, accurate and scalable read mapping by seed-and-vote. *Nucleic Acids Res.* **41**, e108.
- Lindsten, T., and Thompson, C.B. (2006). Cell death in the absence of Bax and Bak. *Cell Death Differ.* **13**, 1272–1276.
- Lindsten, T., Ross, A.J., King, A., Zong, W.X., Rathmell, J.C., Shiels, H.A., Ulrich, E., Waymire, K.G., Mahar, P., Frauwirth, K., et al. (2000). The combined functions of proapoptotic Bcl-2 family members bak and bax are essential for normal development of multiple tissues. *Mol. Cell* **6**, 1389–1399.
- Lum, J.J., Bauer, D.E., Kong, M., Harris, M.H., Li, C., Lindsten, T., and Thompson, C.B. (2005). Growth factor regulation of autophagy and cell survival in the absence of apoptosis. *Cell* **120**, 237–248.
- Mackay, F., Woodcock, S.A., Lawton, P., Ambrose, C., Baetscher, M., Schneider, P., Tschopp, J., and Browning, J.L. (1999). Mice transgenic for BAFF develop lymphocytic disorders along with autoimmune manifestations. *J. Exp. Med.* **190**, 1697–1710.
- Maraskovsky, E., O'Reilly, L.A., Teepe, M., Corcoran, L.M., Peschon, J.J., and Strasser, A. (1997). Bcl-2 can rescue T lymphocyte development in interleukin-7 receptor-deficient mice but not in mutant rag-1<sup>-/-</sup> mice. *Cell* **89**, 1011–1019.
- Martins, V.C., Busch, K., Juraeva, D., Blum, C., Ludwig, C., Rasche, V., Laitschka, F., Mastitsky, S.E., Brors, B., Hielscher, T., et al. (2014). Cell competition is a tumour suppressor mechanism in the thymus. *Nature* **509**, 465–470.
- McCarthy, D.J., Chen, Y., and Smyth, G.K. (2012). Differential expression analysis of multifactor RNA-Seq experiments with respect to biological variation. *Nucleic Acids Res.* **40**, 4288–4297.
- McDonnell, T.J., Deane, N., Platt, F.M., Nunez, G., Jaeger, U., McKearn, J.P., and Korsmeyer, S.J. (1989). bcl-2-immunoglobulin transgenic mice demonstrate extended B cell survival and follicular lymphoproliferation. *Cell* **57**, 79–88.
- Morata, G., and Ripoll, P. (1975). Minutes: mutants of *Drosophila* autonomously affecting cell division rate. *Dev. Biol.* **42**, 211–221.
- Moreaux, J., Legouffe, E., Jourdan, E., Quittet, P., Rème, T., Lugagne, C., Moine, P., Rossi, J.F., Klein, B., and Tarte, K. (2004). BAFF and APRIL protect myeloma cells from apoptosis induced by interleukin 6 deprivation and dexamethasone. *Blood* **103**, 3148–3157.
- Muri, J., Thut, H., Bornkamm, G.W., and Kopf, M. (2019). B1 and Marginal Zone B Cells but Not Follicular B2 Cells Require Gpx4 to Prevent Lipid Peroxidation and Ferroptosis. *Cell Rep.* **29**, 2731–2744.e4.
- Nakano, K., and Voudsen, K.H. (2001). PUMA, a novel proapoptotic gene, is induced by p53. *Mol. Cell* **7**, 683–694.
- Nie, Y., Waite, J., Brewer, F., Sunshine, M.J., Littman, D.R., and Zou, Y.R. (2004). The role of CXCR4 in maintaining peripheral B cell compartments and humoral immunity. *J. Exp. Med.* **200**, 1145–1156.
- Novak, A.J., Bram, R.J., Kay, N.E., and Jelinek, D.F. (2002). Aberrant expression of B-lymphocyte stimulator by B chronic lymphocytic leukemia cells: a mechanism for survival. *Blood* **100**, 2973–2979.
- Novak, A.J., Darce, J.R., Arendt, B.K., Harder, B., Henderson, K., Kindsvogel, W., Gross, J.A., Greipp, P.R., and Jelinek, D.F. (2004). Expression of BCMA, TACI, and BAFF-R in multiple myeloma: a mechanism for growth and survival. *Blood* **103**, 689–694.
- Oliver, E.R., Saunders, T.L., Tarlé, S.A., and Glaser, T. (2004). Ribosomal protein L24 defect in belly spot and tail (Bst), a mouse minute. *Development* **131**, 3907–3920.
- Oltersdorf, T., Elmore, S.W., Shoemaker, A.R., Armstrong, R.C., Augeri, D.J., Belli, B.A., Bruncko, M., Deckwerth, T.L., Dinges, J., Hajduk, P.J., et al. (2005). An inhibitor of Bcl-2 family proteins induces regression of solid tumours. *Nature* **435**, 677–681.

- Opferman, J.T. (2008). Apoptosis in the development of the immune system. *Cell Death Differ.* *15*, 234–242.
- Otipoby, K.L., Sasaki, Y., Schmidt-Supprian, M., Patke, A., Gareus, R., Pasparakis, M., Tarakhovskiy, A., and Rajewsky, K. (2008). BAFF activates Akt and Erk through BAFF-R in an IKK1-dependent manner in primary mouse B cells. *Proc. Natl. Acad. Sci. USA* *105*, 12435–12438.
- Palm, W., and Thompson, C.B. (2017). Nutrient acquisition strategies of mammalian cells. *Nature* *546*, 234–242.
- Patke, A., Mecklenbräuer, I., Erdjument-Bromage, H., Tempst, P., and Tarakhovskiy, A. (2006). BAFF controls B cell metabolic fitness through a PKC beta- and Akt-dependent mechanism. *J. Exp. Med.* *203*, 2551–2562.
- Pillai, S., Cariappa, A., and Moran, S.T. (2005). Marginal zone B cells. *Annu. Rev. Immunol.* *23*, 161–196.
- Quah, B.J., and Parish, C.R. (2012). New and improved methods for measuring lymphocyte proliferation in vitro and in vivo using CFSE-like fluorescent dyes. *J. Immunol. Methods* *379*, 1–14.
- Raff, M.C. (1992). Social controls on cell survival and cell death. *Nature* *356*, 397–400.
- Rahman, Z.S., and Manser, T. (2004). B cells expressing Bcl-2 and a signaling-impaired BAFF-specific receptor fail to mature and are deficient in the formation of lymphoid follicles and germinal centers. *J. Immunol.* *173*, 6179–6188.
- Rathmell, J.C., Vander Heiden, M.G., Harris, M.H., Frauwirth, K.A., and Thompson, C.B. (2000). In the absence of extrinsic signals, nutrient utilization by lymphocytes is insufficient to maintain either cell size or viability. *Mol. Cell* *6*, 683–692.
- Rathmell, J.C., Fox, C.J., Plas, D.R., Hammerman, P.S., Cinalli, R.M., and Thompson, C.B. (2003). Akt-directed glucose metabolism can prevent Bax conformation change and promote growth factor-independent survival. *Mol. Cell Biol.* *23*, 7315–7328.
- Rauch, M., Tussiwand, R., Bosco, N., and Rolink, A.G. (2009). Crucial role for BAFF-BAFF-R signaling in the survival and maintenance of mature B cells. *PLoS ONE* *4*, e5456.
- Ritchie, M.E., Phipson, B., Wu, D., Hu, Y., Law, C.W., Shi, W., and Smyth, G.K. (2015). limma powers differential expression analysis for RNA-sequencing and microarray studies. *Nucleic Acids Res.* *43*, e47.
- Robinson, M.D., and Oshlack, A. (2010). A scaling normalization method for differential expression analysis of RNA-seq data. *Genome Biol.* *11*, R25.
- Robinson, M.D., McCarthy, D.J., and Smyth, G.K. (2010). edgeR: a Bioconductor package for differential expression analysis of digital gene expression data. *Bioinformatics* *26*, 139–140.
- Rolink, A.G., Andersson, J., and Melchers, F. (1998). Characterization of immature B cells by a novel monoclonal antibody, by turnover and by mitogen reactivity. *Eur. J. Immunol.* *28*, 3738–3748.
- Rolink, A.G., Tschopp, J., Schneider, P., and Melchers, F. (2002). BAFF is a survival and maturation factor for mouse B cells. *Eur. J. Immunol.* *32*, 2004–2010.
- Sakai, T., Nishikori, M., Tashima, M., Yamamoto, R., Kitawaki, T., Takaori-Kondo, A., Suzuki, T., Tsuzuki, S., and Uchiyama, T. (2009). Distinctive cell properties of B cells carrying the BCL2 translocation and their potential roles in the development of lymphoma of germinal center type. *Cancer Sci.* *100*, 2361–2367.
- Sasaki, Y., Casola, S., Kutok, J.L., Rajewsky, K., and Schmidt-Supprian, M. (2004). TNF family member B cell-activating factor (BAFF) receptor-dependent and -independent roles for BAFF in B cell physiology. *J. Immunol.* *173*, 2245–2252.
- Sasaki, Y., Derudder, E., Hobeika, E., Pelanda, R., Reth, M., Rajewsky, K., and Schmidt-Supprian, M. (2006). Canonical NF-kappaB activity, dispensable for B cell development, replaces BAFF-receptor signals and promotes B cell proliferation upon activation. *Immunity* *24*, 729–739.
- Schiemann, B., Gommerman, J.L., Vora, K., Cachero, T.G., Shulga-Morskaya, S., Dobles, M., Frew, E., and Scott, M.L. (2001). An essential role for BAFF in the normal development of B cells through a BCMA-independent pathway. *Science* *293*, 2111–2114.
- Shulga-Morskaya, S., Dobles, M., Walsh, M.E., Ng, L.G., MacKay, F., Rao, S.P., Kalled, S.L., and Scott, M.L. (2004). B cell-activating factor belonging to the TNF family acts through separate receptors to support B cell survival and T cell-independent antibody formation. *J. Immunol.* *173*, 2331–2341.
- Smulski, C.R., and Eibel, H. (2018). BAFF and BAFF-Receptor in B Cell Selection and Survival. *Front. Immunol.* *9*, 2285.
- Spanopoulou, E., Roman, C.A., Corcoran, L.M., Schlissel, M.S., Silver, D.P., Nemazee, D., Nussenzweig, M.C., Shinton, S.A., Hardy, R.R., and Baltimore, D. (1994). Functional immunoglobulin transgenes guide ordered B-cell differentiation in Rag-1-deficient mice. *Genes Dev.* *8*, 1030–1042.
- Strasser, A. (2005). The role of BH3-only proteins in the immune system. *Nat. Rev. Immunol.* *5*, 189–200.
- Strasser, A., Harris, A.W., Vaux, D.L., Webb, E., Bath, M.L., Adams, J.M., and Cory, S. (1990). Abnormalities of the immune system induced by dysregulated bcl-2 expression in transgenic mice. *Curr. Top. Microbiol. Immunol.* *166*, 175–181.
- Strasser, A., Harris, A.W., and Cory, S. (1991a). bcl-2 transgene inhibits T cell death and perturbs thymic self-censorship. *Cell* *67*, 889–899.
- Strasser, A., Whittingham, S., Vaux, D.L., Bath, M.L., Adams, J.M., Cory, S., and Harris, A.W. (1991b). Enforced BCL2 expression in B-lymphoid cells prolongs antibody responses and elicits autoimmune disease. *Proc. Natl. Acad. Sci. USA* *88*, 8661–8665.
- Strasser, A., Harris, A.W., Corcoran, L.M., and Cory, S. (1994). Bcl-2 expression promotes B- but not T-lymphoid development in scid mice. *Nature* *368*, 457–460.
- Strasser, A., Puthalakath, H., O'Reilly, L.A., and Bouillet, P. (2008). What do we know about the mechanisms of elimination of autoreactive T and B cells and what challenges remain. *Immunol. Cell Biol.* *86*, 57–66.
- Su, G.H., Chen, H.M., Muthusamy, N., Garrett-Sinha, L.A., Baunoch, D., Tenen, D.G., and Simon, M.C. (1997). Defective B cell receptor-mediated responses in mice lacking the Ets protein, Spi-B. *EMBO J.* *16*, 7118–7129.
- Sun, S.C. (2017). The non-canonical NF- $\kappa$ B pathway in immunity and inflammation. *Nat. Rev. Immunol.* *17*, 545–558.
- Takeuchi, O., Fisher, J., Suh, H., Harada, H., Malynn, B.A., and Korsmeyer, S.J. (2005). Essential role of BAX, BAK in B cell homeostasis and prevention of autoimmune disease. *Proc. Natl. Acad. Sci. USA* *102*, 11272–11277.
- Tang, M.L., Steeber, D.A., Zhang, X.Q., and Tedder, T.F. (1998). Intrinsic differences in L-selectin expression levels affect T and B lymphocyte subset-specific recirculation pathways. *J. Immunol.* *160*, 5113–5121.
- Tardivel, A., Tinel, A., Lens, S., Steiner, Q.G., Sauberli, E., Wilson, A., Mackay, F., Rolink, A.G., Beermann, F., Tschopp, J., and Schneider, P. (2004). The antiapoptotic factor Bcl-2 can functionally substitute for the B cell survival but not for the marginal zone B cell differentiation activity of BAFF. *Eur. J. Immunol.* *34*, 509–518.
- Tasdemir, E., Maiuri, M.C., Galluzzi, L., Vitale, I., Djavaheri-Mergny, M., D'Amelio, M., Criollo, A., Morselli, E., Zhu, C., Harper, F., et al. (2008). Regulation of autophagy by cytoplasmic p53. *Nat. Cell Biol.* *10*, 676–687.
- Thomas, M.D., Kremer, C.S., Ravichandran, K.S., Rajewsky, K., and Bender, T.P. (2005). c-Myb is critical for B cell development and maintenance of follicular B cells. *Immunity* *23*, 275–286.
- Tsujimoto, Y., Finger, L.R., Yunis, J., Nowell, P.C., and Croce, C.M. (1984). Cloning of the chromosome breakpoint of neoplastic B cells with the t(14;18) chromosome translocation. *Science* *226*, 1097–1099.
- Vaux, D.L., Cory, S., and Adams, J.M. (1988). Bcl-2 gene promotes haemopoietic cell survival and cooperates with c-myc to immortalize pre-B cells. *Nature* *335*, 440–442.
- Vikström, I.B., Slomp, A., Carrington, E.M., Moesbergen, L.M., Chang, C., Kelly, G.L., Glaser, S.P., Jansen, J.H., Leusen, J.H., Strasser, A., et al. (2016). MCL-1 is required throughout B-cell development and its loss sensitizes specific B-cell subsets to inhibition of BCL-2 or BCL-XL. *Cell Death Dis.* *7*, e2345.
- Villunger, A., Michalak, E.M., Coultas, L., Müllauer, F., Böck, G., Auserlechner, M.J., Adams, J.M., and Strasser, A. (2003). p53- and drug-induced

apoptotic responses mediated by BH3-only proteins puma and noxa. *Science* 302, 1036–1038.

Warnatz, K., Salzer, U., Rizzi, M., Fischer, B., Gutenberger, S., Böhm, J., Kienzler, A.K., Pan-Hammarström, Q., Hammarström, L., Rakhmanov, M., et al. (2009). B-cell activating factor receptor deficiency is associated with an adult-onset antibody deficiency syndrome in humans. *Proc. Natl. Acad. Sci. USA* 106, 13945–13950.

Wei, M.C., Zong, W.X., Cheng, E.H., Lindsten, T., Panoutsakopoulou, V., Ross, A.J., Roth, K.A., MacGregor, G.R., Thompson, C.B., and Korsmeyer, S.J. (2001). Proapoptotic BAX and BAK: a requisite gateway to mitochondrial dysfunction and death. *Science* 292, 727–730.

Weih, F., Carrasco, D., Durham, S.K., Barton, D.S., Rizzo, C.A., Ryseck, R.P., Lira, S.A., and Bravo, R. (1995). Multiorgan inflammation and hematopoietic abnormalities in mice with a targeted disruption of RelB, a member of the NF-kappa B/Rel family. *Cell* 80, 331–340.

Wilhelmson, A.S., Lantero Rodriguez, M., Stubelius, A., Fogelstrand, P., Johansson, I., Buechler, M.B., Lianoglou, S., Kapoor, V.N., Johansson, M.E., Fagman, J.B., et al. (2018). Testosterone is an endogenous regulator of BAFF and splenic B cell number. *Nat. Commun.* 9, 2067.

Woodland, R.T., Fox, C.J., Schmidt, M.R., Hammerman, P.S., Opferman, J.T., Korsmeyer, S.J., Hilbert, D.M., and Thompson, C.B. (2008). Multiple signaling pathways promote B lymphocyte stimulator dependent B-cell growth and survival. *Blood* 111, 750–760.

Wu, D., Lim, E., Vaillant, F., Asselin-Labat, M.L., Visvader, J.E., and Smyth, G.K. (2010). ROAST: rotation gene set tests for complex microarray experiments. *Bioinformatics* 26, 2176–2182.

Youle, R.J., and Strasser, A. (2008). The BCL-2 protein family: opposing activities that mediate cell death. *Nat. Rev. Mol. Cell Biol.* 9, 47–59.

Young, M.D., Wakefield, M.J., Smyth, G.K., and Oshlack, A. (2010). Gene ontology analysis for RNA-seq: accounting for selection bias. *Genome Biol.* 11, R14.

## STAR★METHODS

### KEY RESOURCES TABLE

REAGENT or RESOURCE	SOURCE	IDENTIFIER
<b>Antibodies</b>		
Pacific Blue anti-mouse/human CD45R/B220 Antibody	Biolegend	Cat#103227; RRID:AB_492876
PE anti-mouse BAFF-R (7H22-E16) Antibody	Biolegend	Cat#134103; RRID:AB_1626160
PE anti-mouse CD4 (GK1.5) Antibody	Biolegend	Cat#100408; RRID:AB_312693
PE/Cy7 anti-mouse CD8a (53-6.7) Antibody	Biolegend	Cat#100722; RRID:AB_312761
FITC anti-mouse CD21(7E9) Antibody	Biolegend	Cat#123408; RRID:AB_940403
PE anti-mouse CD23 (B3B4) Antibody	Biolegend	Cat#101608; RRID:AB_312833
FITC anti-mouse/human CD44 (IM7) Antibody	Biolegend	Cat#103006; RRID:AB_312957
APC/Cy7 anti-mouse CD45.1 (A20) Antibody	Biolegend	Cat#110716; RRID:AB_313505
Brilliant Violet 785 anti-mouse CD45.2 (104) Antibody	Biolegend	Cat#109839; RRID:AB_2562604
APC anti-mouse CD62L (MEL-14) Antibody	Biolegend	Cat#104412; RRID:AB_313099
PE/Cy7 anti-mouse CD71(RI7217) Antibody	Biolegend	Cat#113812; RRID:AB_2203382
PE anti-mouse CD98 (4F2) Antibody	Biolegend	Cat#128207; RRID:AB_1186107
Brilliant Violet 421 anti-mouse CXCR5 (L138D7) Antibody	Biolegend	Cat#145511; RRID:AB_2562127
PE anti-mouse TACI (8F10) Antibody	Biolegend	Cat#133403; RRID:AB_2240584
APC anti-mouse TCR $\beta$ chain (H57-597) Antibody	Biolegend	Cat#109211; RRID:AB_313434
PE-Cyanine7 CD19 Antibody (1D3)	eBioscience	Cat#25-0193-82; RRID:AB_657663
Biotin Anti-CD19 Antibody (1D3)	BD Biosciences	Cat# 553784; RRID:AB_395048
FITC Anti-IgM Antibody (II/41)	BD Biosciences	Cat# 553437; RRID:AB_394857
APC anti-mouse CD93 Antibody (AA4.1)	BioLegend	Cat# 136510; RRID:AB_2275868
APC anti CXCR4 Antibody (2B11)	Thermo Fisher Scientific	Cat# 17-9991-80; RRID:AB_10670877
eFluor 450 anti CD93 Antibody (AA4.1)	Thermo Fisher Scientific	Cat# 48-5892-80; RRID:AB_2574084
FITC anti-BCMA Antibody (161616)	R and D Systems	Cat# FAB593F; RRID:AB_2256028
eFluor 450 Streptavidin	Thermo Fisher Scientific	Cat# 48-4317-82; RRID:AB_10359737
Brilliant Violet 785 Streptavidin	BioLegend	Cat#405249
Alexa Fluor 700 Streptavidin	Thermo Fisher Scientific	Cat#S21383
Biotin anti-mouse/human CD45R/B220 antibody (RA3-6B2)	Biolegend	Cat# 103204; RRID:AB_312989
Biotin anti-mouse CD3 antibody (17.A2)	Biolegend	Cat# 100244; RRID:AB_2563947
Biotin anti-mouse CD4 antibody (GK1.5)	Biolegend	Cat# 100404; RRID:AB_312689
Biotin anti-mouse CD8a antibody (53.6.7)	Biolegend	Cat# 100704; RRID:AB_312743
Biotin anti-mouse F4/80 antibody (BM8)	BioLegend	Cat# 123106; RRID:AB_893501
Biotin anti-mouse Gr-1 antibody (RB6-8C5)	BioLegend	Cat# 108404; RRID:AB_313369
Biotin anti-mouse NK-1.1 antibody (PK136)	BioLegend	Cat# 108704; RRID:AB_313391
APC anti-mouse TER-119 antibody (TER-119)	BioLegend	Cat# 116212; RRID:AB_313713
APC anti-mouse CD117 antibody (2B8)	BioLegend	Cat# 105812; RRID:AB_313221
PE/Cy7 anti-mouse Sca-1 antibody (D7)	BioLegend	Cat# 108114; RRID:AB_493596
Pacific Blue anti-BrdU Antibody (MoBU-1)	Thermo Fisher Scientific	Cat# B35129; RRID:AB_2536433
Goat anti-mouse IgG3 HRP (polyclonal)	Southern Biotech	Cat # 1100-05; RRID: AB_2794573
Goat anti-mouse IgM HRP (polyclonal)	Southern Biotech	Cat # 1020-05; RRID: AB_2794201
Purified anti-B220 antibody (clone RA3-6B2)	WEHI antibody facility	N/A
Purified anti-CD19 antibody (clone 1D3)	WEHI antibody facility	N/A

(Continued on next page)

**Continued**

REAGENT or RESOURCE	SOURCE	IDENTIFIER
Purified anti-rat IgG antibody (clone TIB216)	WEHI antibody facility	N/A
FITC Anti-IgM Antibody (II/41)	BD Biosciences	Cat#550676; RRID:AB_398464
Purified Anti-IgM Antibody (II-41)	BD Biosciences	Cat#553435; RRID:AB_394855
Biotin Anti-IgD Antibody (11-26)	Origene	Cat#AM08012BT-N; RRID:AB_1873226
Purified Anti-CD21 Antibody (SC0681)	Invitrogen	Cat#MA5-32227; RRID:AB_2809513
Donkey anti-Rabbit IgG Alexa Fluor Plus 647	Thermo Fisher Scientific	Cat# A32795; RRID:AB_2762835
Streptavidin, Alexa Fluor 568	Thermo Fisher Scientific	Cat# S-11226; RRID:AB_2315774
Donkey anti-Rat IgG Alexa Fluor 488	Thermo Fisher Scientific	Cat# A-21208; RRID:AB_2535794

**Biological samples**

Rat serum	Sigma	R9759
-----------	-------	-------

**Chemicals, peptides, and recombinant proteins**

5-Bromo-2'-deoxyuridine	Sigma	Cat#B5002
recombinant human BAFF	PeproTech	Cat#310-13
Paraformaldehyde	Sigma	Cat#158127
TWEEN® 20	Sigma	Cat#P1379
RNase-Free DNase	Promega	Cat#M6101
ABT-737	Active Biochem	Cat#A-1002
L-asparagine	Sigma	Cat#A4159
L-Arg-HCl	Sigma	Cat#A5131
Glycine	Sigma	Cat#G5417
L-Serine	Sigma	Cat#S4500
L-Tyrosine disodium salt dihydrate	Sigma	Cat#RES3156T-A701X
L-Histidine monohydrochloride monohydrate	Sigma	Cat#H8125
L-Isoleucine	Sigma	Cat#I2752
L-Leucine	Sigma	Cat#L8000
L-Lysine monohydrochloride	Sigma	Cat#L8662
L-Methionine	Sigma	Cat#M9625
L-Phenylalanine	Sigma	Cat#P5482
L-Threonine	Sigma	Cat#T8625
L-Tryptophan	Sigma	Cat#T0254
L-Valine	Sigma	Cat#V0500
L-Glutamine	Sigma	Cat#G8540
2-Mercaptoethanol	Sigma	Cat#M3148
L-Cystine dihydrochloride	Sigma	Cat#C6727
D-Glucose	Sigma	Cat#G7021
Cyclohexamide	Sigma	Cat#C7698
Leptomycin B	Sigma	Cat#L2913
Antimycin A	Sigma	Cat#A8674
Oligomycin	Selleck	Cat#S1478
Actinomycin D	Sigma	Cat#A9415
Cell Trace Violet	Invitrogen	Cat#C34557
Perm/Wash Buffer	BD Biosciences	Cat#554723
Cytofix/Cytoperm buffer	BD Biosciences	Cat#554722
OPD-substrate solution	Sigma	Cat#P9187
NBT/BCIP Stock Solution	Sigma	Cat#11681451001
Bovine Serum Albumine (cell culture)	PAA laboratories	Cat#K51-001
Propidium iodide	Sigma	Cat#P4864

(Continued on next page)

**Continued**

REAGENT or RESOURCE	SOURCE	IDENTIFIER
<b>Critical commercial assays</b>		
QIAamp DNA Blood Mini Kit	QIAGEN	Cat#51104
RNeasy extraction Mini kit	QIAGEN	Cat#74104
DreamTaq Green PCR Master Mix	Thermo Fisher Scientific	Cat#K1081
<b>Deposited data</b>		
RNA-sequencing data	This paper	GSE158475
<b>Experimental models: organisms/strains</b>		
Mouse: <i>Bak1</i> KO	<a href="#">Lindsten et al., 2000</a>	RRID:MGI:2656013
Mouse: BAFF Tg	<a href="#">Mackay et al., 1999</a>	MGI:2386944
Mouse: <i>Tnfrsf13c</i> KO	<a href="#">Sasaki et al., 2004</a>	RRID:MGI:3716689
Mouse: <i>Rag1</i> KO	<a href="#">Spanopoulou et al., 1994</a>	MGI:2448994
Mouse: <i>Nfkb2</i> KO	<a href="#">Franzoso et al., 1998</a>	MGI:2179705
Mouse: <i>Relb</i> KO	<a href="#">Weih et al., 1995</a>	MGI:2179545
Mouse: <i>Spib</i> KO	<a href="#">Su et al., 1997</a>	MGI:2448991
Mouse: floxed <i>Bax</i>	<a href="#">Takeuchi et al., 2005</a>	MGI:3589203
Mouse: floxed <i>Myb</i>	<a href="#">Emambokus et al., 2003</a>	MGI:3037362
Mouse: floxed <i>Tpr53</i>	<a href="#">Jonkers et al., 2001</a>	MGI:2156651
Mouse: <i>CD23-Cre</i> Tg	<a href="#">Kwon et al., 2008</a>	MGI:3803652; RRID:IMSR_JAX:028197
<b>Oligonucleotides</b>		
FWD-Bxfl	Integrated DNA Technologies	ACTAGGCCCGGTCCAAGAAC
RVS-Bxfl	Integrated DNA Technologies	GAATGCCAAAAGCAAACAGACC
RVS-del	Integrated DNA Technologies	GGCCCCAAAACCTCAGCTAC
<b>Software and algorithms</b>		
Flowjo (Treestar)	FlowJo, LLC	<a href="https://www.flowjo.com/">https://www.flowjo.com/</a>
Prism, version 8	Graph Pad	<a href="https://www.graphpad.com/scientific-software/prism/">https://www.graphpad.com/scientific-software/prism/</a>
ImageJ	National Institutes of Health (NIH)	<a href="https://imagej.nih.gov/ij/">https://imagej.nih.gov/ij/</a>
<b>Other</b>		
Anti-Biotin MicroBeads	Miltenyi Biotec Inc.	Cat#130-090-485
LS Columns	Miltenyi Biotec Inc.	Cat#130-042-401
CalIBRITE APC Beads	BD Biosciences	Cat#340487
Microtainer tubes containing EDTA	Sarstedt	Cat#20.1341.100
Ficoll-Paque PLUS	Cytiva	Cat#17-1440-02
DMEM	GIBCO	Cat#11885084
DMEM No Glucose	GIBCO	Cat#11966025
DMEM, high glucose	GIBCO	Cat#10313021
DMEM without Amino Acids	US Biological Life Sciences	Cat#D9800-13

**RESOURCE AVAILABILITY**

**Lead contact**

Further information and requests for resources and reagents should be directed to and will be fulfilled by the lead contact, Stéphane Chappaz ([stephane.chappaz@monash.edu](mailto:stephane.chappaz@monash.edu)).

**Materials availability**

The mouse lines generated in this study may be obtained (pending continued availability) from the lead contact with a completed materials transfer agreement.

### Data and code availability

- RNA-seq data have been deposited at GEO and are publicly available as of the date of publication via accession number GEO: GSE158475.
- All methods used to analyze these data are publicly available in the open-source R packages referred to the methods.
- Any additional information required to reanalyze the data reported in this paper is available from the lead contact upon request.

## EXPERIMENTAL MODEL AND SUBJECT DETAILS

### Mice

Animals were bred and maintained at The Walter and Eliza Hall Institute of Medical Research Animal Facility and at Monash University in specific pathogen-free facilities. Experiments were conducted as sex unbiased, with mice randomly assigned to experimental groups. All mice used for *in vivo* and *in vitro* experiments were between 10 and 12 weeks of age unless specified otherwise. Mice carrying the CD23-Cre Tg (Kwon et al., 2008), the BAFF Tg (Mackay et al., 1999), the germline deletion of *Bak1* (Lindsten et al., 2000), *Tnfrsf13c* (Sasaki et al., 2004), *Rag1* (Spanopoulou et al., 1994), *Nfkb2* (Franzoso et al., 1998), *Relb* (Weih et al., 1995), *Spib* (Su et al., 1997) or the floxed alleles of *Bax* (Takeuchi et al., 2005), *Myb* (Emambokus et al., 2003) and *Trp53* (Jonkers et al., 2001) have been previously described. All lines were maintained on a C57BL/6 genetic background.

### Animal experiments

All animal experiments complied with the regulatory standards of, and were approved by, the Animal Ethics Committees of The Walter and Eliza Hall Institute (WEHI) and Monash University. For quantification of spleen and LN lymphocyte populations, tissues were homogenized between two glass slides and cells enumerated by flow cytometry with CaliBRITE beads (BD Biosciences). For analysis of LNs in cKO mice and chimeric mice, inguinal, brachial and axillary LNs were pooled together. Automated blood cell counts were performed on blood collected from the retro-orbital plexus into Microtainer tubes containing EDTA (Sarstedt) using an Advia 2120 hematological analyzer (Siemens). For BM chimera experiments, Ly5.1<sup>+</sup> recipients were lethally irradiated (2x 5.5 Gy) before being reconstituted with 5x10<sup>6</sup> Ly5.2<sup>+</sup> BM donor cells. Chimeras were analyzed 8 weeks after transplantation. For antibody mediated cell depletion experiments, antibodies were generated in the WEHI antibody facility. *Bak1*<sup>-/-</sup> *Bax*<sup>fl/fl</sup> CD23-Cre mice received i.v. injections of 150 μg of monoclonal antibodies against B220 (clone RA3-6B2) and CD19 (clone 1D3) on day 0 followed by i.v. injection of 150 μg monoclonal anti-rat IgG antibody (clone TIB216) on day 2. Lymphoid compartments were analyzed at day 4 using antibodies against IgM (clone II/41) and CD23 (clone B3B4) for identifying Fo B cells. For experiments with recombinant cytokine, 5 μg of human BAFF (PreproTech) or saline were injected i.v. into *Bak1*<sup>-/-</sup> *Bax*<sup>fl/fl</sup> CD23-Cre mice for two consecutive days before analysis. For adoptive transfer experiments, peripheral LNs and spleens from WT and *Bak1*<sup>-/-</sup> *Bax*<sup>fl/fl</sup> CD23-Cre donor animals were first stained with biotinylated monoclonal antibodies against CD19 (clone 1D3) and then incubated with magnetic anti-Biotin beads (Miltenyi Biotec). CD19<sup>+</sup> B cells were then positively selected on MACS columns (Miltenyi Biotec), enumerated by flow cytometry and mixed at 1:1 ratio. These cell suspensions were CTV-labeled as previously described (Quah and Parish, 2012). Briefly, cells were resuspended in RPMI medium supplemented with 10% fetal calf serum (SIGMA) at a concentration of 100x10<sup>6</sup> cells per mL and stained with 80 μM CTV (Invitrogen) for 5 min at room temperature. Cells were then washed 3 times and approximately 5x10<sup>6</sup> CTV-labeled cells were injected i.v. per recipient. The cells of different origin (test, competitor and recipient) all carried unique combinations of the congenic Ly5.1 and Ly5.2 markers. At the indicated time points, spleen and inguinal LNs of the recipients were analyzed by flow cytometry. For immunization, NP<sub>55</sub>-Ficoll was diluted in sterile PBS to a final concentration of 40 μg/100 μL and administered to each mouse i.p.. Mice were analyzed 5 days post-immunisation.

## METHOD DETAILS

### Flow cytometry

Flow cytometric acquisition of data was performed with BD Biosciences LSR, FACSCanto II, Fortessa, FACS Verse and FACS Calibur analyzers. Acquisition for Fo B cell phenotyping was done on an Aurora (Cytek) machine with autofluorescence removal. Flow Jo software was used for data analysis. Organ cellularity and *in vitro* cell counts were determined by flow cytometry by adding a known number of APC-labeled CaliBRITE beads (BD Biosciences) to samples. Blood-borne lymphocytes were purified with Ficoll-Paque PLUS (Cytiva). Relative cell size for *ex vivo* and *in vitro* experiments was obtained from the ratio between forward light scatter of viable cells and CaliBRITE beads. Antibodies for flow cytometry and cell sorting were labeled with FITC, PE, PE-Cy7, APC, Alexa Fluor 700, APC-Cy7, Pacific Blue, eFluor450 and biotin. Antibodies against B220 (RA3-6B2), BAFFR (7H22-E16), CD4 (GK1.5), CD8a (53.6.7), CD21 (7E9), CD23 (B3B4), CD44 (IM7) CD45.1 (A20), CD45.2 (104), CD62L (MEL14), CD71 (RI7217), CD93 (AA4.1) CD98 (RL388), CD117 (2B8), CXCR5 (L138D7), Sca1 (D7), TACI (8F10) and TCRβ (H57-597) were purchased from Biolegend. Antibodies against CD19 (1D3) and IgM (II/41) were purchased from BD Biosciences. Antibodies against CD93 (AA4.1) and CXCR4 (2B11) were purchased from Thermo Fisher Scientific. The antibody against BCMA (161616) was purchased from R&D systems. As secondary reagents, Streptavidin-eFluor450 (Thermo Fisher Scientific), Streptavidin-BV785 (Biolegend), and Streptavidin-Alexa700 (Molecular

probes) were used. Propidium iodide (PI, Sigma-Aldrich) at a final concentration of 20  $\mu\text{g}/\text{mL}$  was used to exclude dead cells. Cell sorting was done on Influx and FACS Aria (BD Biosciences) cell sorters with > 99.5% purity.

### BrdU labeling in mixed BM chimeric mice

BM cells from 6 individual  $\text{Ly5.2}^+ \text{Bak1}^{-/-} \text{Bax}^{\text{fl/fl}} \text{CD23-Cre}$  (test) donors and from several  $\text{Ly5.1}^+$  WT (competitor) donors were successively stained with biotin-labeled antibodies against lineage markers (B220 (RA3-6B2), CD3 (17.A2), CD4 (GK1.5), CD8a (53.6.7), F4/80 (BM8), Gr1 (RB6-8C5), NK1.1 (PK136), Ter119 (TER-119) purchased from Biolegend and CD19 (1D3) purchased from BD Biosciences) and then incubated with magnetic anti-Biotin beads (Miltenyi Biotech). Lineage<sup>-</sup> progenitors were then negatively selected on MACS columns and viable cells were enumerated by flow cytometry. Each of the 6 progenitor suspensions from a  $\text{Ly5.2}^+ \text{Bak1}^{-/-} \text{Bax}^{\text{fl/fl}} \text{CD23-Cre}$  donor was mixed at 1:9 ratio with the competitor  $\text{Ly5.1}^+$  WT cell suspension. For each mix, the 1 to 9 ratio was confirmed by flow cytometry in lineage<sup>-</sup> c-Kit<sup>+</sup>Sca1<sup>+</sup> cells. Each of these 6 mixed cell suspensions was then used to reconstitute 7  $\text{Ly5.1}^+ \text{Ly5.2}^+$  recipient mice that had previously been irradiated with 900 rad. The following day, the recipients were injected with 40 mg/kg of BrdU (Sigma) and received BrdU (0.8 mg/L) in the drinking water for 6 consecutive weeks. During the chase period, six recipients that had received test cells of distinct origin were analyzed at the indicated time point. Splenocyte numbers were counted by flow cytometry and stained with antibodies against CD19, CD21, CD23, CD45.1, CD45.2 and CD93. They were then fixed overnight in Cytofix/Cytoperm buffer (BD Biosciences) at 4°C, washed once in Perm/Wash buffer (BD Biosciences) and resuspended in 1% PFA (Sigma) 0.5% Tween-20 (Sigma) (v/v) in PBS for 30 min at room temperature. After a single wash in Perm/Wash buffer, cells were fixed a second time in Fix/Perm buffer on ice for 15 min, washed twice in Perm/Wash buffer before being resuspended in 0.15 M NaCl and 4.2 mM  $\text{MgCl}_2$  with 50 U of DNase (Promega). DNase treatment was performed at 37°C for 30 min. Cells were then washed twice in Perm/Wash buffer and stained with an antibody against BrdU (clone MoBU-1, Life Technologies) for 30 min on ice. After 2 washes in Perm/Wash buffer, quantification of BrdU<sup>+</sup> cells of test and competitor origin was done by flow cytometry.

### In vitro assays

For experiments probing cell size regulation, Fo B cells were isolated from peripheral LNs. LN cells were stained with a biotinylated antibody against CD19 and then incubated with anti-Biotin beads (Miltenyi Biotech). Fo B cells were positively selected with LS columns (Miltenyi Biotech) and their purity was routinely > 98%. cKO Fo B cells were plated in 96 well plate U bottom plates (Falcon) in either complete DMEM (GIBCO), sugar-free DMEM (GIBCO) or aa free DMEM (US Biological life sciences) and medium were supplemented with 2% BSA (PAA laboratories) at cell density of  $25 \times 10^3$ – $40 \times 10^3$  cells/well. Dextrose, CHX, LMB, Oligomycin, Antimycin, ActD and all aa (L-Arg-HCl, Glycine, L-serine, L-Tyrosine disodium salt dehydrate, L-Histidine monohydrochloride monohydrate, L-Isoleucine, L-Leucine, L-Lysine monohydrochloride, L-Methionine, L-Phenylalanine, L-Threonine, L-Tryptophan, L-Valine, L-Asparagine, L-Cystine dihydrochloride and L-Glutamine) were purchased from Sigma. Relative cell size was measured after 48 h of culture on a FACS Verse analyzer.

For ABT-737 (inhibitor of BCL-2, BCL-XL and BCL-W) sensitivity and growth factor deprivation assays, splenic B cells were first positively selected via magnetic separation as described above. Magnetically purified splenic B cells were then stained with fluorescently labeled antibodies directed against CD21, CD23, CD93 and Streptavidin. Fo B cells and MZ B cells were then FACS-sorted as  $\text{CD19}^+ \text{CD93}^- \text{CD21}^+ \text{CD23}^+$  and  $\text{CD19}^+ \text{CD93}^- \text{CD21}^{\text{high}} \text{CD23}^{\text{low}}$ , respectively.

For ABT-737 sensitivity assays, sorted Fo and MZ B cells were plated in 96 well plate U bottom plates in the high-glucose version of DMEM supplemented with 250  $\mu\text{M}$  L-asparagine (Sigma), 50  $\mu\text{M}$  2-ME (Sigma) and 10% fetal calf serum in the presence or absence of 10  $\mu\text{M}$  ABT-737 (Active Biochem). The next day,  $10^4$  APC-conjugated CaliBRITE beads (BD Biosciences) and PI (20  $\mu\text{g}/\text{mL}$ ) were added to each well before acquisition of data on a FACS Calibur analyzer for quantification of viable cells.

For GFD assays, FACS-sorted Fo and MZ B cells from  $\text{Ly5.2}^+ \text{Bak1}^{-/-} \text{Bax}^{\text{fl/fl}} \text{CD23-Cre}$  and  $\text{Ly5.1}^+$  WT origin were mixed and plated in 96 well plate U bottom plates in complete DMEM (GIBCO) supplemented with 2% BSA. The same day and for the consecutive three days, quantification of viable cells was performed on a FACS Verse analyzer after addition to each well of  $10^4$  APC-conjugated CaliBRITE beads, PI and antibodies against CD45.1.

### Deletion of the floxed Bax allele

For assessing the deletion of the floxed *Bax* allele, transitional and mature B cells were FACS-sorted from the spleen as T1 ( $\text{CD19}^+ \text{CD93}^+ \text{IgM}^{\text{high}} \text{CD23}^{\text{low}}$ ), T2 ( $\text{CD19}^+ \text{CD93}^+ \text{IgM}^{\text{high}} \text{CD23}^+$ ), T3 ( $\text{CD19}^+ \text{CD93}^+ \text{IgM}^{\text{low}} \text{CD23}^+$ ), Fo ( $\text{CD19}^+ \text{CD93}^- \text{CD21}^+ \text{CD23}^+$ ) and MZ ( $\text{CD19}^+ \text{CD93}^- \text{CD21}^{\text{high}} \text{CD23}^{\text{low}}$ ) B cells. Sorted subsets were used for genomic DNA extraction with QIAamp DNA blood Mini Kit (QIAGEN). PCR analysis was performed on 10 ng of gDNA per sample using the DreamTaq Green PCR Master Mix (Thermo Fisher) under the following conditions: 10 min at 95°C, followed by 30 cycles of 30 s at 95°C, 30 s at 55°C, and 55 s at 72°C. The following primers (FWD-Bxfl ACTAGGCCCGGTCCAAGAAC and RVS-Bxfl GAATGCCAAAAGCAAACAGACC) amplified a 350 bp fragment specific for the undeleted floxed *Bax* allele. The primer (RVS-del GGCCCCAAAACCTCAGCTAC) used in combination with FWD amplified a 863 bp fragment which was specific for the deleted floxed *Bax* allele.

### Transcriptome analyses

Only males were used for isolating cells for transcriptome analysis. BM suspension isolated from tibia and femur of mice were labeled with biotinylated antibodies against CD19 (BD Biosciences) followed by magnetic anti-Biotin beads (Miltenyi Biotech). B cells were

then positively selected on LS columns (Miltenyi Biotech), stained with antibodies against IgM, B220 and CD93 on ice. Recirculating Fo B lymphocytes were flow sorted as B220<sup>high</sup>IgM<sup>+</sup>CD93<sup>-</sup> and were routinely > 99.8% pure. Total RNA was extracted using the RNeasy extraction Mini kit (QIAGEN). The purity of the RNA samples was assessed by Tape station (Agilent). Samples were prepped for RNA-seq analysis using Illumina reagents as per the TruSeq RNA sample preparation v2 Guide (Low Sample 23 Protocol). The completed library was then assessed for quality using the Tape Station (Agilent) and samples were pooled and run on a miSeq sequencer (Illumina).

### Bioinformatics analysis

3 RNA preparations isolated from 3 individual mice were processed for each genotype (*Bak1*<sup>-/-</sup>*Bax*<sup>fl/fl</sup> and *Bak1*<sup>-/-</sup>*Bax*<sup>Δ/Δ</sup>) together with 6 other samples that were not used in this study. Sequencing reads were processed using the R programming language (v3.3.1) and the Rsubread software package (v1.20.3) (Liao et al., 2013). Paired-end reads were aligned to the mm10 genome using the sub-junc function, and then summarized into gene-level counts by the featureCounts function (argument isPairedEnd = TRUE and using in-built mm10 gene annotation). Differential gene expression analysis was then carried out on the counts using an updated version of R (v4.0.1), for reference chromosomes only (chr 1 to 19, and chr X and Y). The counts were pre-processed by keeping only genes (12,677) that were expressed (counts-per-million > 1) in at least 3 samples, and then normalized using the TMM method (Robinson and Oshlack, 2010) in the calcNormFactors function of edgeR v3.30.3 (McCarthy et al., 2012; Robinson et al., 2010). A mixed effects model was fitted to the counts using limma v3.44.1 (Ritchie et al., 2015), with biological groups as fixed effects and sample collection date as random effects.

Briefly, this involved the calculation of precision weights by the voom function (Law et al., 2014), which were then inserted into a calculation of correlation for sample collection date using the duplicateCorrelation function. Both functions were run twice with the insertion of correlation or weight estimates from the previous step. The final model found 251 genes (including *Bax*) to be downregulated between apoptosis refractory and control samples, and 195 genes to be upregulated (adjusted p value cutoff of 5%). For this comparison, we tested whether any “biological process” GO terms have been over-represented using the goana function (Young et al., 2010) in limma. Roast gene set testing (Wu et al., 2010) was also carried out for select gene sets from the Molecular Signatures Database version 7.1, where mouse orthologs were downloaded from <http://bioinf.wehi.edu.au/MSigDB/>. Barcode plots from limma were used to give a visual representation of whether a gene set is enriched in our data. In the plots, genes were ranked by their moderated t-statistics for the comparison between cKO and *Bak1*<sup>-/-</sup>*Bax*<sup>fl/fl</sup> control samples (the blue section marks negative values and the red section marks positive values). Vertical black bars mark the presence of genes that belong to the gene set, where the curve above the barplot indicates an enrichment of genes from the gene set (or high density of black bars) if its value is high.

Raw and processed RNA-seq data are available from GEO under accession number GSE158475.

### ELISA

Quantification of BAFF serum levels was performed by using the Mouse BAFF Quantikine ELISA Kit (R&D Systems) following the manufacturer’s instructions. For detection of NP-specific antibodies, 96-well high binding plates (Sarstedt) were coated overnight at 4°C with 5 μg/μL of NP<sub>12</sub>-BSA for IgG3 antibodies or NP<sub>9</sub>-BSA for IgM antibodies. Plates were blocked the following day for 1 h with PBS-1%BSA, washed with PBS-Tween and distilled water and then loaded, in duplicate, with serum samples from mice immunized with NP-Ficoll. Samples were serially diluted in PBS-1%BSA and incubated for 4 h at 37°C. Plates were then washed in PBS-Tween and distilled water before incubating for 1 h with either IgG3-specific or IgM-specific anti-mouse secondary antibody conjugated to horseradish peroxidase (Southern Biotech). After a final wash with PBS-Tween and distilled water, plates were developed with OPD-substrate solution (Sigma Aldrich).

### ELISpot

Multiscreen HA plates (Millipore) were coated overnight at 4°C, with 10 μg/μL of NP<sub>12</sub>-BSA for IgG3+ secreting cells or NP<sub>9</sub>-BSA for IgM+ secreting cells. Plates were blocked the following day for 1 h with PBS-1%BSA and then washed with PBS. 10<sup>5</sup> splenocytes from each mouse were loaded into the plates in duplicate in RPMI-5%FCS, 50 μM 2-ME and 2 mM Glutamine. The plates were incubated overnight at 37°C, washed the following day with PBS-Tween and distilled water and incubated for 1 h at 37°C with either IgG3-specific or IgM-specific anti-mouse secondary antibody conjugated to alkaline-phosphatase (Southern Biotech). Plates were washed with PBS-Tween and distilled water and developed with the BCiP®/NBT reaction (Sigma-Aldrich).

### Immunofluorescence

Seven-micrometer acetone-fixed spleen sections were incubated with goat serum and then with purified rat anti-IgM (clone II/41, BD PharMingen). Anti-IgM antibody was detected with a donkey anti-rat Alexa 488 antibody (Invitrogen). Sections were then incubated with rat serum (Sigma) and subsequently with purified rabbit anti-CD21 (clone SC0681, Invitrogen) and biotinylated rat anti-IgD (Clone 11-26, Origene) antibodies. Anti-IgD and anti-CD21 antibodies were detected with Streptavidin Alexa 568 (Invitrogen) and donkey anti-rabbit Alexa 647 (Invitrogen), respectively. Images were captured on a Zeiss LSM 980 Confocal Microscope and analyzed with ImageJ software.

#### QUANTIFICATION AND STATISTICAL ANALYSIS

Statistical analyses were performed using Prism software (GraphPad). *P* values were calculated by Student unpaired t test with Welch's correction or by Mann-Whitney nonparametric, two-tailed test as indicated in figure legends. P values are indicated as follows: (\*)  $p < 0.05$ ; (\*\*)  $p < 0.01$ ; (\*\*\*)  $p < 0.001$  and (\*\*\*\*)  $p < 0.0001$ .  $p > 0.05$  is indicated as "NS" (not significant). Variables and sample sizes are indicated in the figure legend.